Journal of Archaeological Science: Reports 17 (2018) 404–421

Contents lists available at ScienceDirect

Journal of Archaeological Science: Reports

journal homepage: www.elsevier.com/locate/jasrep

Volcanic minerals in Chaco Canyon, New Mexico and their archaeological significance

Kenneth Barnett Tankersley[a,b,*], Warren D. Huff[b], Nicholas P. Dunning[c], Lewis A. Owen[b], Vernon L. Scarborough[a]

[a] Department of Anthropology, University of Cincinnati, Cincinnati, OH 45221, USA
[b] Department of Geology, University of Cincinnati, Cincinnati, OH 45221, USA
[c] Department of Geography, University of Cincinnati, Cincinnati, OH 45221, USA

1. Introduction

Sunset Crater, Arizona, a ~340 m cinder cone composed of loose pyroclastic clinkers and scoria, is one of the youngest volcanoes in North America. The most recent eruptions of Sunset Crater occurred during the late Holocene, ~1085 CE (Hanson, 2017), a date that falls within the Pueblo II cultural period. These eruptions are thought to have been Strombolian in type, which resulted in the deposition of a layer of ash and lapilli over ~2100 km^2 (Elson et al., 2011a, 2011b). In this paper we provide the first evidence of anonymously high levels of Ni, Cr, and Pt, and volcanogenic mineral phenocrysts in alluvial strata from Chaco Canyon, New Mexico, which date to the time of Sunset Crater's most recent eruption, some 325 km WSW of Chaco Canyon. We also discuss the implications of this eruption on Ancestral Puebloan culture.

1.1. Chaco Canyon

Chaco Canyon is located in northwestern New Mexico near the Four Corners region of the southwestern United States. A significant portion of the canyon lies within the Chaco Culture National Historical Park, which is managed by the National Park Service under the auspices of the United States Department of the Interior and in cooperation with the park's American Indian Consultation Committee. Chaco Culture National Historical Park, together with Aztec Ruins, a National Monument, and five nearby and contemporary archaeological sites managed by the United States Bureau of Land Management including Casamero, Halfway House, Kin Nizhoni, Pierre, Salmon Ruins, and Twin Angels, constitute the UNESCO Chaco Culture World Heritage site (Lekson, 2005).

Archaeological sites in Chaco Canyon span > 13,000 years of prehistory with the most intensive (~4000 people) and well-studied occupation dating to the Ancestral Puebloan Bonito Phase, between ~850 CE to 1140 (Vivian, 1990; Plog, 2012; Vivian and Hilpert, 2012). The archaeological sites from this period include a dense concentration of sandstone masonry pueblos (Great Houses) and kivas, 15 of which are among the largest pre-Nineteenth century buildings in North America (Strutin, 1994). An extensive network of canals, dams, furrowed fields, gates, and reservoirs supplied ample water to maize grown in the fertile soils of akchin, dune, and gridded agricultural fields (e.g., Marshall et al., 1979; Vivian, 1990; Dean and Funkhouser, 2002; Vivian et al., 2006; Wills and Dorshow, 2012; Cully and Toll, 2015; Vivian and Watson, 2015; Tankersley et al., 2017; Tankersley, 2017).

1.2. Geologic setting

Chaco Canyon is located in the San Juan Basin, an asymmetric structural depression in the Colorado Plateau province on the western side of the Continental Divide. The canyon is formed in the Cliffhouse Sandstone and Menefee Formation, which make up a portion of the Cretaceous Mesa Verde Group and date to ~80 Ma (Scott et al., 1984). The Chaco Wash and its tributaries (Gallo and Fajada Washes), the Escavada Wash, and numerous rincons dissecting the canyon walls drain the canyon and adjacent lands (Fig. 1). Rincons are narrow alcoves and secluded rim-rock drainages, many of which occur in the Cretaceous Cliff House Sandstone and underlying Menefee Formation on the north side of Chaco Canyon east of the confluence with Escavada Wash. The basal deposits of the rincons are filled with fine-grained sheet-wash, aeolian sand, and gravelly alluvial sand from seasonal snowmelt and rainwater runoff across the Cliff House Sandstone and overlying aeolian sand and the Jeddito Formation (Scott et al., 1984).

The Escavada Wash watershed covers ~600 km^2 (Fig. 1), within the larger Arizona-New Mexico Plateau ecological region, which encompasses ~190,000 km^2 ranging in elevation from 660 to 3640 m above mean sea level (amsl) (Vivian and Hilpert, 2012). The Escavada Wash originates in the Lybrook Badlands on the western side of the Continental Divide and the Cretaceous-Tertiary (K-T) stratigraphic boundary. The Cretaceous Lewis Shale Formation (~35 m) that consists of light-brown sandstone, and light gray to olive-gray claystone, sandstone, siltstone, and sandy concretionary limestone is cut through the

* Corresponding author at: Department of Anthropology, PO Box 210380, 481 Braunstein Hall, University of Cincinnati, Cincinnati, OH 45221-0380, USA.
E-mail address: kenneth.tankersley@uc.edu (K.B. Tankersley).

https://doi.org/10.1016/j.jasrep.2017.11.027
Received 24 July 2017; Received in revised form 12 November 2017; Accepted 20 November 2017

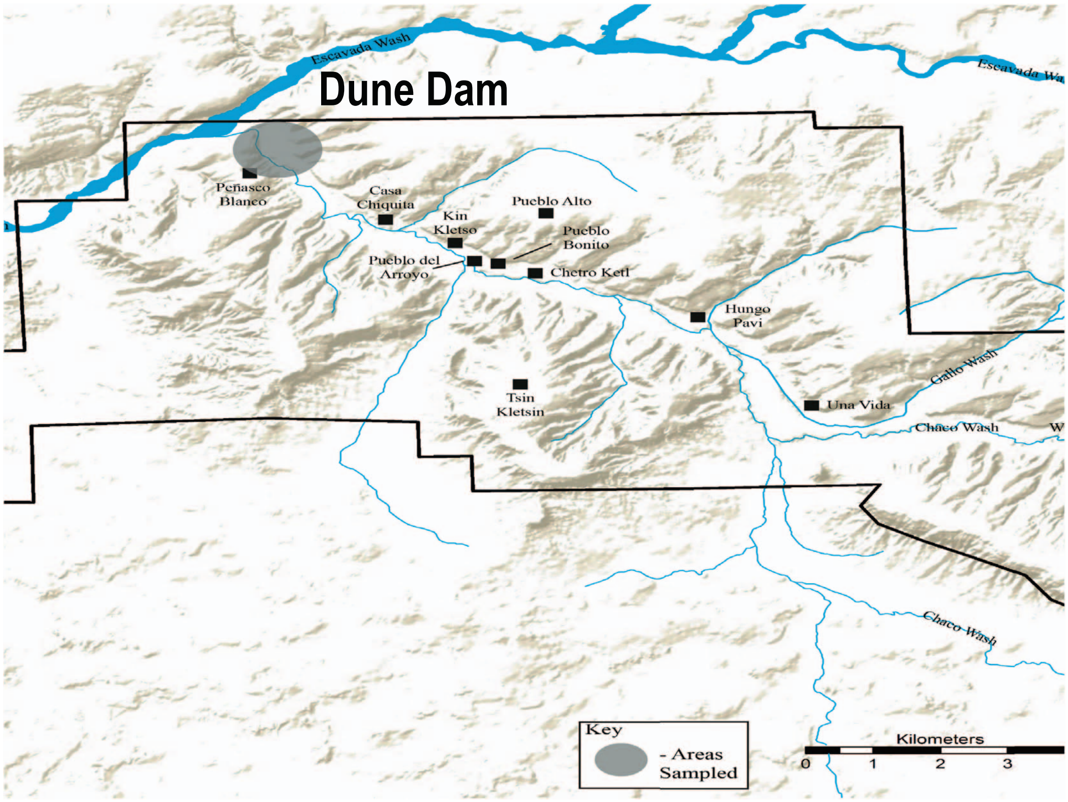

Fig. 1. Map of Chaco Canyon, New Mexico showing the location of the Dune Dam area. (After Tankersley et al., 2017).

Escavada Wash (Scott et al., 1984). The undifferentiated alluvium deposits of the late Holocene Naha and Tsegi formations overlie the Lewis Shale along much of the drainage. The Naha Formation is composed of a grayish brown, friable, thinly to cross-bedded, discontinuous sand and silt, while the Tsegi Formation consists of yellowish gray-to-gray brown, consolidated fine to coarse sand, silt, and clay (Scott et al., 1984; Haussner, 2016).

The Chaco Wash watershed, including the tributary Gallo and Fajada washes, covers ~3850 km^2 and ranges in elevation from 1860 to 2040 m amsl. Water flows westward from Star Lake on a strongly jointed, light-colored, mica-rich quartzite and through the Upper Cretaceous Cliff House Sandstone Formation. The Cliff House Formation exposed along Chaco Wash is composed of massive (~130 m) white-to-dark yellowish-orange, fine to coarse-grained sandstone, and gray-to-brown carbonaceous shale (Scott et al., 1984). In the Escavada Wash confluence area, the Chaco Wash also cuts through the Menefee Formation that includes a thick (~475 m) sequence of grayish-yellow to brown, fine to medium grained cross-bedded sandstone with inclusive beds of dusky-yellow to olive-gray sandy shale and mudstone, brown sandy limestone, carbonaceous shale, and coal (Scott et al., 1984).

Quaternary deposits include a well-developed, high-level, late Pleistocene alluvial terrace, 18–60 m above the Chaco Wash. This terrace consists of dark yellowish brown to grayish orange chert, quartz, and sandstone gravel and pebbles (Scott et al., 1984). A lower, late Pleistocene to early Holocene alluvial terrace (Jeddito Formation) consists of angular yellow-brown cobble- to pebble-size chert, petrified wood, sandstone, siderite, quartzite, and quartz (Scott et al., 1984). Undifferentiated late Holocene Naha and Tsegi alluvium are laterally adjacent to the Jeddito Formation and comparable in composition to late Holocene alluvium exposed in the Escavada Wash (Scott et al., 1984). Poorly consolidated alluvium consisting of clay, silt, and coarse to medium sand with pebble to slab-size rock fragments derived from the canyon walls occurs laterally to the Naha and Tsegi sediments (Scott et al., 1984). Portions of all of these sediments are covered by colluvium, talus, and aeolian sand. Cut and fill channels and alluvial fans are locally abundant within Chaco Canyon (Lekson, 2005; Haussner, 2016).

1.3. Volcanogenic minerals

Geologically, the Quaternary sediments of Chaco Canyon are derived entirely from the weathering and erosion of Cretaceous sedimentary rocks. However, volcanogenic minerals have been found in late Holocene archaeological contexts including a roughly spherical and partially drilled pyrope garnet (Specimen CHCU 18488) from an unnamed archaeological site, 29SJ116, and a "sizeable and unworked" garnet (Specimen USNM 336036) from Room 330 in Pueblo Bonito, site 29SJ387, (Judd, 1954; Eveleth and Lueth, 2010). Additionally, trachyte tempered pottery has been identified in Chaco Canyon and is thought to have originated from the eastern footslope of the Chuska Mountain range, also known as the Chuska Slope or Chuska Valley, New Mexico (King, 2003). Trachyte is an alkali feldspar-rich igneous rock, which contains biotite, clinopyroxene, and olivine.

During the summer months of 2013, Vernon Scarborough extracted a solid sediment core from the late Holocene alluvium in Chaco Canyon near the confluence with Escavada Wash (which we refer to here as the Dune Dam area). The core was extracted from the floodplain of Chaco Wash immediately below Peñasco Blanco, a circular Ancestral Puebloan Great House constructed ~900 CE and 1125 and near a pictograph thought to portray the sighting of the 1054 CE supernova (Kelley and Milone, 2004). Because the age of the Peñasco Blanco site complex overlaps with the most recent proposed volcanic eruptions of Sunset

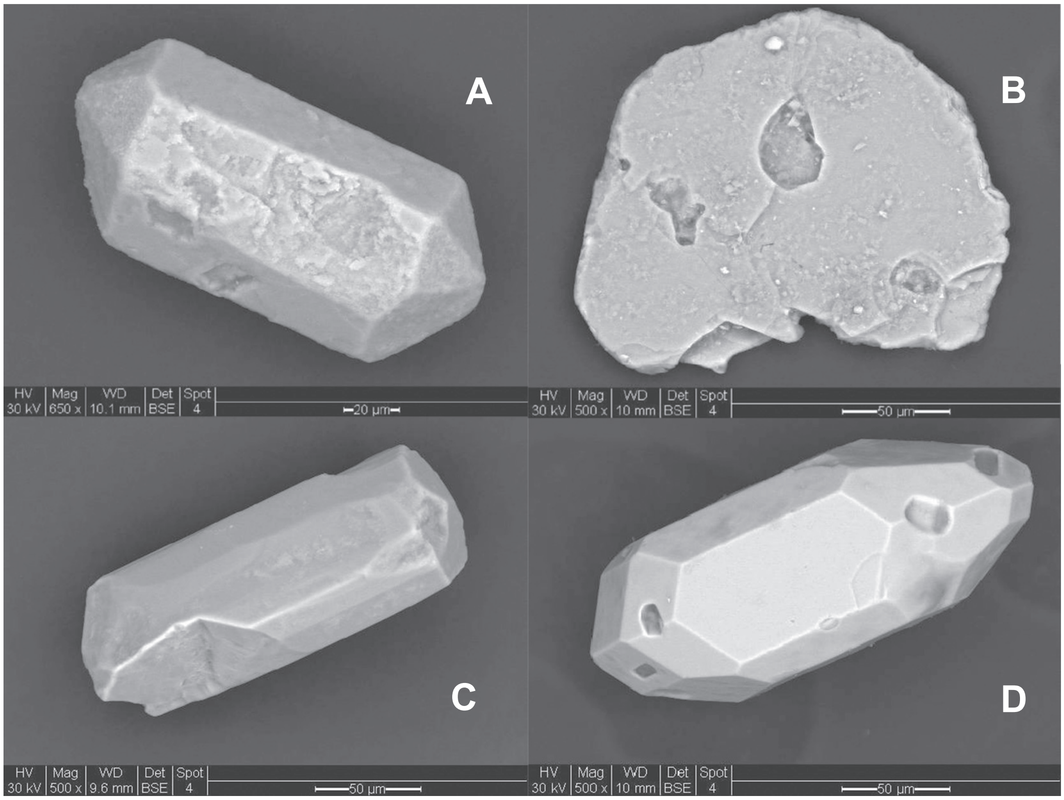

Fig. 2. Environmental scanning electron micrographs of volcanogenic minerals from the 2013 Dune Dam core: A. apatite, B. biotite; C. clinopyroxene, D. Zircon. (After Haussner et al., 2015).

Crater in Arizona (Hanson et al., 2008a; Hanson et al., 2008b; Elson et al., 2011a; Elson et al., 2011b; Hanson, 2017), the sediments were microscopically examined for volcanogenic minerals. Apatite, biotite, clinopyroxene, and zircon were found concentrated in three levels: 50–75 cm, 90–179 cm, and 199–233 cm below the surface (Fig. 2). Additionally, X-ray diffractometry demonstrated that smectite, a product of weathered volcanic glass, co-occurred with the volcanogenic mineral phenocrysts. While this initial discovery was tantalizing and suggested that felsic volcanic ash from Sunset Crater may have fallen on Chaco Canyon, there were other explanations including other volcanic eruptions in western North America that may have resulted in felsic ash falls. (Haussner et al., 2015).

While Sunset Crater represents the most recent volcanic eruption in western North America, there were earlier volcanic eruptions that may have produced a felsic ash fall. Indeed, Chaco Canyon is located within the proposed geographic distributions of the Lava Creek B (~0.64 Ma), Mesa Falls (~1.29 Ma), and Huckleberry Ridge ash falls (~2.06 Ma) (Yellowstone Caldera), Bishop ash fall (~0.76 Ma, Long Valley Caldera), Guaje Pumice and Otowi ash fall (~1.14 Ma, Toledo Caldera), and the Tsankawi and Tshirege ash fall (~1.50 Ma, Bandelier Valles Caldera) (Bailey et al., 1969; Izett et al., 1970; Christiansen and Blank, 1972; Wilcox and Naeser, 1992). If the volcanogenic minerals resulted from one or more of these earlier catastrophic volcanic events, then the age of the volcanic mineral phenocrysts recovered from the late Holocene sediments of the Dune Dam area would be between somewhere between 0.64 and 2.06 Ma (Haussner et al., 2015).

2. Methods

2.1. Field methods

To determine whether the volcanic mineral phenocrysts in Chaco Canyon dated to the late Holocene or sometime between 0.639 ± 0.002 and 2.059 ± 0.004 Ma, samples were collected from late Holocene alluvium and Ancestral Puebloan hydraulic deposits in the Dune Dam area in 2015. Fifty-five sediment samples spanning > 3000 years were collected from test unit excavations, cut bank profile excavations, solid sediment cores, and the alluvium of Chaco Wash and its tributaries, the Gallo and Fajada Washes, Escavada Wash, and Rincons on the eastern side of the canyon (Tankersley et al., 2017). Additionally, samples were collected from natural exposures of the Mesa Verde Group to determine if volcanogenic minerals were present in the Cretaceous bedrock.

A portable JMC hand-operated soil sampler was used to extract 15 cores in the floodplain near the Chaco-Escavada Wash confluence area. Following the methods discussed by Tankersley et al. (2016a, 2017), a 3-cm-diameter and 1 m-long stainless steel core-tubes were pounded into the ground using a 5 kg slide-hammer to a depth of 3 m or to refusal. Samples were collected directly into clear, PETG co-polyester liners with red (top) and black (bottom) color-coded vinyl caps.

Sediment samples were also collected from a cut bank profile on an exposure of the Chaco Wash floodplain and three test units, one in the Chaco Wash floodplain and two on the periphery of the Chaco Wash floodplain and Rincon alluvium. All of the sediment was hand dug and processed through 0.25 cm screens. Sedimentary units were labeled based according to their stratigraphic sequence and soils were characterized using Munsell soil color, sedimentary and ped-structures, and particle size.

2.2. X-ray diffractometry (XRD)

Whole rock samples of Cretaceous age bedrock were prepared for XRD. Initially, they were air-dried and powdered for random particle orientation and mounting as a pressed powder. Samples were ground

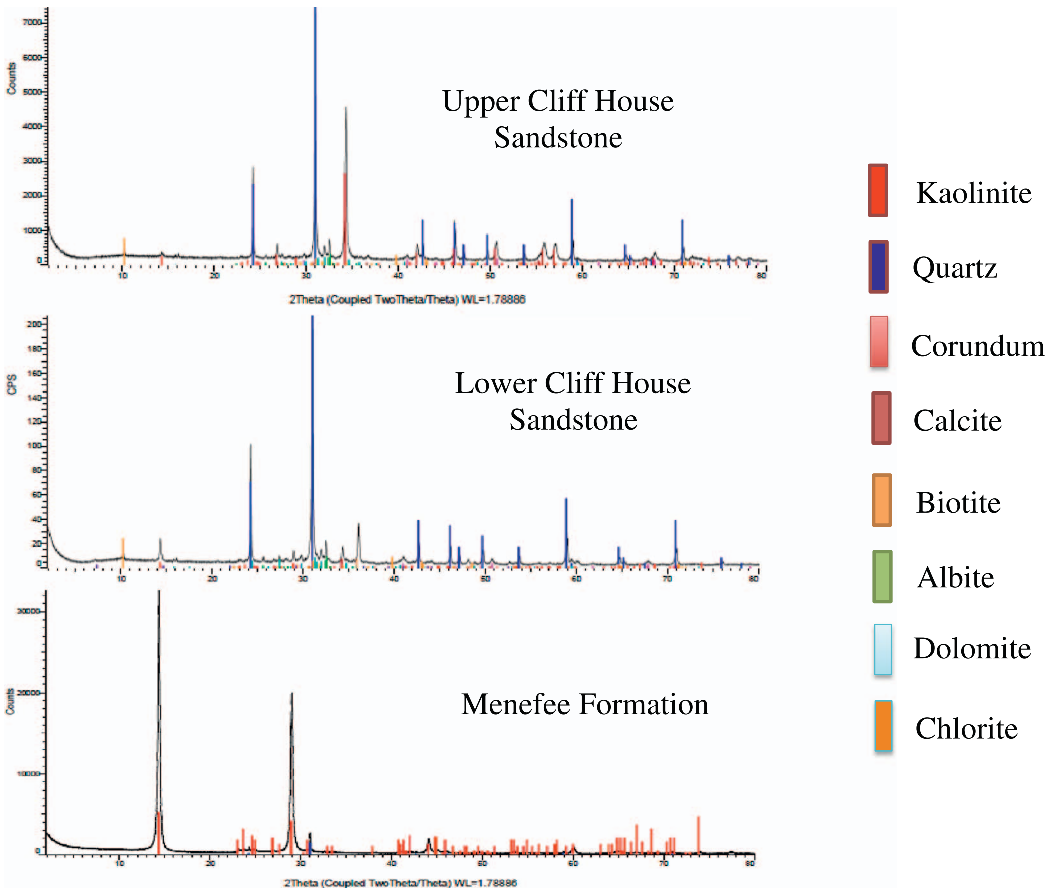

Fig. 3. X-ray diffractograms of Cretaceous bedrock from Chaco Canyon.

for 10 min in a McCrone Micronizing mill using corundum pucks to achieve particle size of < 5 μm. XRD data was collected using a Bruker D8 Advance diffractometer. Instrument conditions included using CoKa radiation (generated at 35 kV and 40 mA), 260 mm goniometer radius, 0.6 mm primary slit, Fe-filter, and a Lynx-Eye position sensitive solid-state detector. XRD scan parameters were run at 0.3 s/step in 0.01 Æ2θ step increments. Data was processed using Bruker Eva software, which includes background correction, Ka2 stripping and peak D-spacing and intensity assignments.

The bulk mineral composition of alluvium and sediment samples from an Ancestral Puebloan canal was identified using XRD. To minimize preferred orientation problems and narrow particle-size distribution, 2–4 ml aliquots were air-dried and ground to a powder in a McCrone XRD-Mill. A 125 ml polypropylene container was filled with an ordered array of 48 cylindrical grinding elements to preserve crystal lattices during grinding. To optimize micronization, grinding time of the aliquots varied between 3 and 30 min depending on the range in particle sizes. Desiccated and powdered XRD samples were scanned with 2θ from 2° to 68° on a Rigaku MiniFlex XRD system using a CoKα radiation source. XRD was conducted at 25 °C with a step-time of 15.4 s. Minerals were identified on the basis of 2θ peak position and peak intensity (Lin Count) by matching resulting peaks with the International Crystal Diffraction Database (ICDD).

2.3. Energy dispersive X-ray fluorescence spectrometry (ED-XRF)

Minor and trace element mass fractions of alluvium and sediment samples from an Ancestral Puebloan canal were determined by ED-XRF following the procedures described in Tankersley (2017). Samples were prepared using the pressed powder pellet method described by Ingham and Starbuck (1995) and more recently by Hunt et al. (2014). Approximately 10 g of powdered sediment were mixed with 2 ml of Elvacite acrylic resin dissolved in a mixture of 1 l of acetone and 200 g of Elvacite powder.

Aliquots were thoroughly mixed in a mortar and pestle for a period between 5 to 10 min depending upon the time needed to homogenize the sample. This mixture was placed into a 40 mm aluminum sample cup and placed in a pellet-press die and compressed using a hydraulic press between 1.59–1.72 × 10^{-8} Pa for 3 min. A controlled pressure release over a period between 30 and 60 s provided a consistent analytical surface (Hunt et al., 2014).

Minor and trace element analysis of the powder pressed aliquots were conducted on a ThermoScientific ARL Quant'X ED-XRF analyzer. The aliquots were excited using a Rh tube with a Be end window. Following the methods described by Shackley (2011) and Hunt et al. (2014), dispersed X-rays were collected using a Si drift detector. The effects of Compton scatter peak were reduced by automatically adjusting the X-ray flux and current setting so the count rate and dead time of ~50% was achieved (Hunt et al., 2014).

2.4. Inductively coupled plasma mass spectrometry (ICP-MS)

Platinum group element analysis was accomplished using ICP-MS. Selected sediment samples from the Ancestral Puebloan canal were

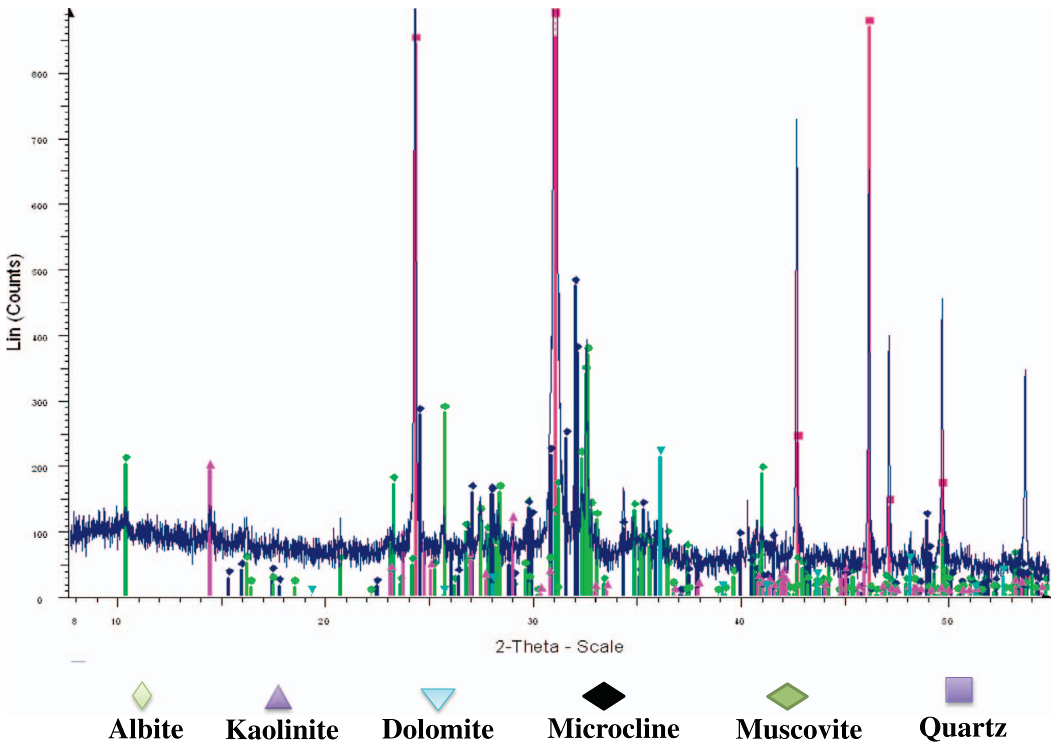

Fig. 4. X-ray diffractogram of Rincon alluvium.

transferred to pre-weighed digestion vessels. Aqua Regia was added to the samples at a ratio of 5:1 (aqua regia/sample). The samples were then warmed in a heating block at 90 °C for 1 h. After cooling, the samples were diluted with 18 MΩ water. Aliquots were analyzed by ICP-MS (PQ Excell). Calibration standards were analyzed and a full quantitative analysis of samples was performed.

2.5. Environmental scanning electron microscopy (ESEM) and energy-dispersive X-ray spectroscopy (EDS)

Sediment samples were sieved between 74 and 250 μm and subjected to LST (lithium metatungstate and diiodomethane) heavy liquid density separation to obtain volcanic mineral phenocrysts. Handpicked aliquots were then examined and photographed with an ESEM and chemically analyzed using EDS.

3. Results

3.1. X-ray diffractometry

XRD peaks in Å using standard descriptors characterized all minerals (Brindley and Brown, 1980). Major minerals in bedrock samples from the Menefee Formation include kaolinite and quartz (Fig. 3). Bedrock samples from the Upper and Lower Cliff House Sandstone Formation contain albite, biotite, calcite, chlorite, dolomite, kaolinite, and quartz (Fig. 3). Corundum was also identified in bedrock samples from the Cliff House Formation and may be the result of contamination during the micronizing step of the sample preparation procedure. Albite, kaolinite, microcline, muscovite, and quartz were present in all of the alluvium samples (Figs. 4, 5, 6). Dolomite was found in sediment samples from Chaco Wash and the adjacent Rincons, but not those from Escavada Wash (compare Figs. 4, 5, 6). Vermiculite was found in sediment samples from the Escavada Wash and Chaco Wash, but not in the Rincons.

3.2. Energy dispersive X-ray fluorescence spectrometry

Minor elements (Na, Mg, Al, Si, P, K, Ca, Ti, Mn, Fe) were measured as oxides at the percent level (Tables 1 and 2) and trace elements (As, Ba, Co, Cr, Cu, Nb, Ni, Pb, Rb, Sr, Th, U, V, Y, Zn, Zr) were measured at the ppm (Tables 3 and 4). With the exception of sediment samples C-03 B, C-03 C2, and C-01 C4, the mean percent composition of all of the sediment samples are comparable to those obtained from alluvium in the Chaco Wash and its tributaries the Gallo and Fajada Washes, the Escavada Wash, and Rincons (compare Tables 1 and 3, and Tables 2 and 4). The minor elements Na, Ti, K, and Fe were anomalously low in samples C-03 B, C-03 C2, and C-01 C4. The percent composition of Na and Ti were below detection limits, K was ≤ 0.17%, and Fe was 0.22% (Table 2, Fig. 7). Conversely, the trace elements Cr and Ni were anomalously high in samples C-03 B, C-03 C2, and C-01 C4. The Cr content was 1668–1875 ppm and Ni was 18,717–23,408 ppm (Table 4, Fig. 8).

3.3. Inductively coupled plasma mass spectrometry

A high quantity of Pt was found in sediment sample C-03 B (43.6 ppb). A control sediment sample from contemporary alluvium in the non-volcanic region of the lower Little Miami River valley, Ohio, some 2250 km east of Chaco Canyon was also examined for Pt. It had a Pt content of 0.6 ppb, which is well within the expected range of Pt from alluvium that did not contain mafic, felsic, or intermediate volcanogenic mineral phenocrysts.

3.4. Energy-dispersive X-ray spectroscopy (EDS) and environmental scanning electron microscopy (ESEM)

Scanning electron micrographs and EDS of crystalline minerals were found to be consistent with amphibole, biotite, epidote, ilmenite, olivine, and zircon mafic and felsic volcanogenic mineral phenocrysts

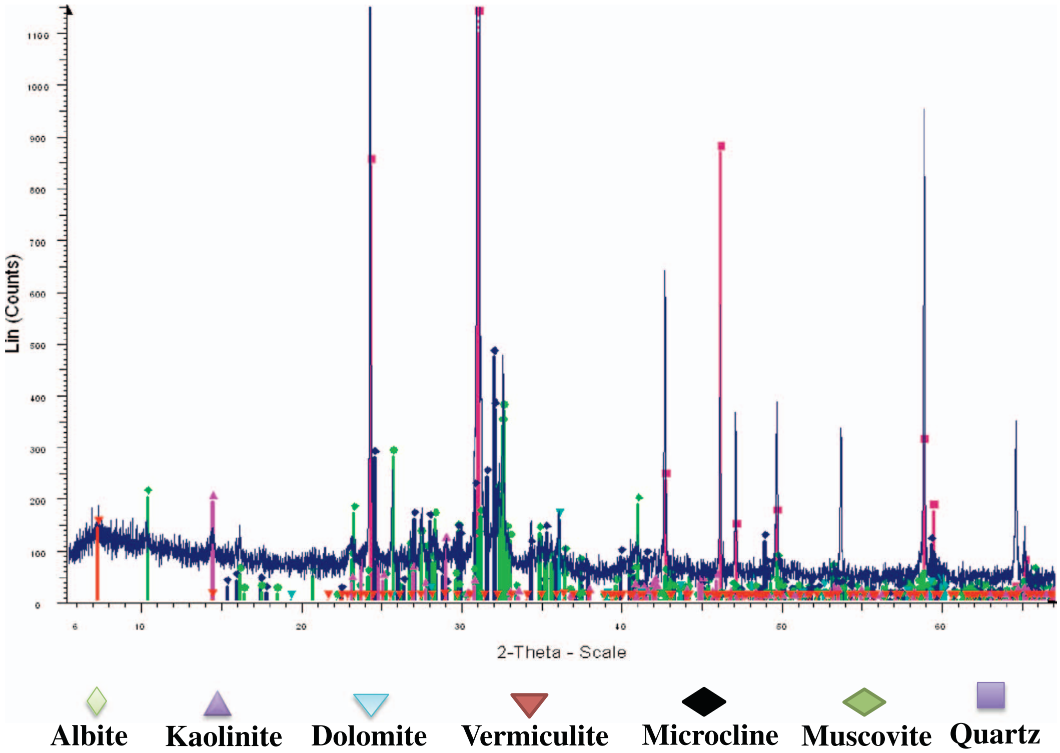

Fig. 5. X-ray diffractogram of Chaco Wash alluvium.

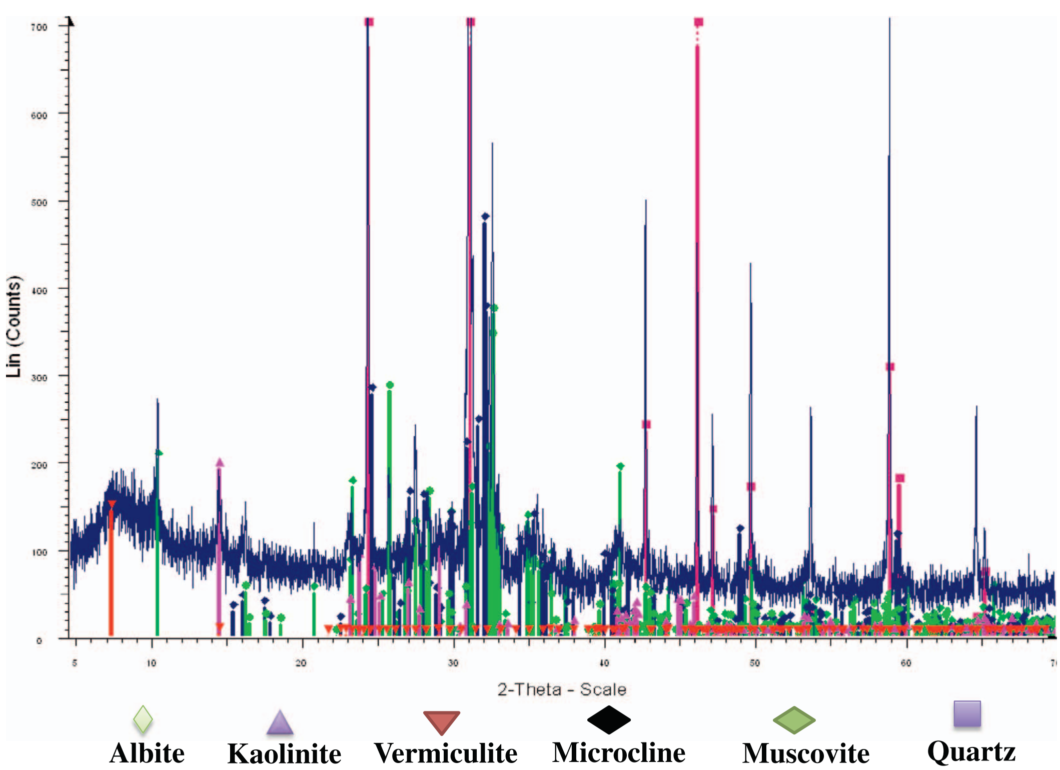

Fig. 6. X-ray diffractogram of Escavada Wash alluvium.

Table 1
Minor element percent composition of sediments from the Chaco Wash, Escavada Wash, and Rincons.

Alluvium	Na_2O	MgO	Al_2O_3	SiO_2	P_2O5	K_2O	CaO	TiO_2	MnO	Fe_2O_3
Rincon 1	1.04	1.33	10.95	78.60	0.265	2.21	2.97	0.477	0.032	2.14
	0.82	1.30	10.91	78.91	0.247	2.20	2.93	0.499	0.031	2.17
	1.07	1.31	10.83	78.75	0.241	2.21	2.93	0.476	0.029	2.16
Mean	0.98	1.31	10.89	78.75	0.251	2.21	2.94	0.484	0.031	2.16
Rincon 3	1.21	1.63	15.08	71.29	0.229	2.67	4.01	0.642	0.043	3.30
	1.09	1.65	15.10	71.27	0.243	2.70	4.03	0.637	0.040	3.31
	1.19	1.61	15.04	71.35	0.221	2.67	4.02	0.644	0.045	3.30
Mean	1.16	1.63	15.07	71.30	0.231	2.68	4.02	0.641	0.043	3.31
Rincon 4	0.84	1.53	15.23	72.59	0.216	2.40	3.68	0.542	0.049	3.00
	0.81	1.58	15.28	72.42	0.246	2.40	3.76	0.561	0.045	2.99
	0.71	1.52	15.20	72.70	0.221	2.39	3.74	0.542	0.040	3.02
Mean	0.79	1.54	15.23	72.57	0.228	2.40	3.73	0.548	0.045	3.00
Chaco F	0.82	1.23	13.07	73.04	0.218	2.48	4.89	0.514	0.095	3.68
	0.69	1.26	13.14	73.03	0.218	2.49	4.92	0.509	0.095	3.70
	0.73	1.24	13.00	73.16	0.2	2.49	4.94	0.499	0.100	3.69
Mean	0.75	1.24	13.07	73.08	0.212	2.48	4.92	0.507	0.097	3.69
Chaco G	1.02	1.12	13.12	77.33	0.202	2.45	2.28	0.422	0.024	2.03
	0.83	0.92	13.04	77.77	0.193	2.45	2.30	0.454	0.023	2.04
	0.82	0.96	12.94	77.79	0.193	2.47	2.30	0.450	0.026	2.05
Mean	0.89	1.00	13.03	77.63	0.196	2.46	2.29	0.442	0.024	2.04
Rincon 5	1.38	1.55	11.79	76.38	0.237	2.38	3.56	0.437	0.032	2.29
	0.89	1.48	11.94	76.74	0.242	2.38	3.61	0.450	0.028	2.29
	0.95	1.51	11.77	76.83	0.227	2.41	3.55	0.482	0.034	2.29
Mean	1.07	1.51	11.83	76.65	0.235	2.39	3.57	0.457	0.031	2.29
Escavada 3	1.62	0.65	12.97	77.58	0.202	2.27	1.24	0.804	0.056	2.73
	1.69	0.71	13.03	77.38	0.19	2.28	1.25	0.799	0.052	2.73
	1.63	0.67	12.98	77.58	0.184	2.26	1.22	0.803	0.056	2.74
Mean	1.65	0.68	12.99	77.51	0.192	2.27	1.23	0.802	0.055	2.73
Chaco 1	1.05	1.20	14.71	74.87	0.215	2.38	2.04	0.721	0.045	2.88
	1.26	1.23	14.77	74.57	0.209	2.37	2.07	0.744	0.044	2.87
	1.01	1.14	14.72	74.98	0.185	2.37	2.05	0.717	0.046	2.89
Mean	1.10	1.19	14.73	74.81	0.203	2.37	2.06	0.727	0.045	2.88
Escavada 1	1.61	0.66	12.86	77.92	0.199	2.31	1.21	0.813	0.050	2.49
	1.57	0.69	12.84	77.98	0.195	2.29	1.21	0.796	0.053	2.50
	1.46	0.60	12.71	78.27	0.187	2.30	1.24	0.806	0.053	2.50
Mean	1.55	0.65	12.80	78.05	0.194	2.30	1.22	0.805	0.052	2.50
Escavada 2	1.52	0.69	13.05	77.68	0.176	2.32	1.22	0.804	0.048	2.63
	1.52	0.70	13.10	77.62	0.178	2.30	1.23	0.779	0.058	2.62
	1.58	0.70	13.00	77.66	0.173	2.32	1.23	0.778	0.052	2.62
Mean	1.54	0.70	13.05	77.65	0.176	2.31	1.23	0.787	0.053	2.62

(Fig. 9, Table 5). This mineral mix suggests they were the result of an intermediate volcanic ash fall.

4. Discussion

4.1. Volcanogenic minerals in Chaco Canyon

The Cretaceous was one of the most volcanically active geologic periods in the history of the planet. Not surprisingly, the sedimentary rocks of the Cretaceous Mesa Verde Group (i.e., Cliff House and Menefee Formation) exposed in Chaco Canyon contains the minerals feldspar (albite), kaolinite, mica (biotite and chlorite), and quartz, which are derived from the weathering of igneous rocks. Similarly, the alluvium of Chaco Wash and its tributaries, the Escavada Wash, and Rincons contain feldspar (albite and associated microcline), kaolinite, and mica (muscovite and vermiculite). Vermiculite is a weathering product of biotite.

In addition to igneous rock forming minerals in the bedrock and alluvium of Chaco Canyon, there is direct positive evidence of at least one and perhaps as many as three late Holocene volcanic ash-falls. The presence of the clay mineral smectite in the late Holocene sediments of the Dune Dam area demonstrates that volcanic ash is present in Chaco Canyon. Volcanogenic mineral phenocrysts, including amphibole, biotite, epidote, ilmenite, olivine, and zircon were also identified in the late Holocene sediments of the Dune Dam area. They are absent in the Cretaceous bedrock and present-day alluvium derived from that bedrock. While biotite occurs in the local bedrock, the pepper-like particulate biotite found in association with the other volcanogenic mineral phenocrysts suggests an airborne volcanic ash origin rather than a by-product of weathering sandstone.

In the Dune Dam area, volcanic mineral phenocrysts occur in the same strata, which produced the anomalously high concentrations of Ni, Cr, and Pt. While these trace elements can be elevated in sediments associated with hydrothermal activity, neither hot springs nor faults are present in Chaco Canyon (Scott et al., 1984). Similarly, Ni, Cr, and Pt can be elevated in chondrite-rich sediments (Moore et al., 2017). However, magnetic microspherules and microtektites commonly associated with chondrite-rich sediments are conspicuously absent. The anomalously high Ni, Cr, and Pt are most likely associated with the volcanogenic mineral phenocrysts such as olivine (Schreiber, 1979).

Table 2
Minor elements percent composition of sediments from the Dune Dam area.

Sub-op unit[a]	Na_2O	MgO	Al_2O_3	SiO_2	P_2O_5	K_2O	CaO	Ti	MnO	Fe_2O_3
C-03 L	0.79	0.96	9.88	58.03	0.18	1.97	1.44	0.550	0.040	2.05
	1.02	0.98	9.99	59.04	0.17	1.99	1.49	0.530	0.040	2.04
	0.62	0.89	9.76	58.20	0.16	1.97	1.48	0.530	0.040	2.04
Mean	0.81	0.94	9.88	58.42	0.17	1.98	1.47	0.540	0.040	2.04
C-03 B	0.00	0.51	28.78	20.12	0.16	0.17	0.34	0.000	0.320	0.22
	0.00	0.45	29.17	20.14	0.15	0.17	0.33	0.000	0.320	0.22
	0.00	0.38	29.16	20.12	0.15	0.16	0.33	0.000	0.330	0.22
Mean	0.00	0.45	29.04	20.13	0.15	0.17	0.33	0.000	0.320	0.22
C-03 C1	1.28	1.18	16.23	59.32	0.15	1.41	1.55	0.700	0.050	5.62
	1.64	1.16	16.22	59.46	0.15	1.44	1.58	0.670	0.050	5.61
	1.17	1.06	16.03	59.22	0.15	1.41	1.59	0.670	0.050	5.60
Mean	1.36	1.13	16.16	59.34	0.15	1.42	1.57	0.680	0.050	5.61
C-03 C2	0.00	0.40	24.97	20.32	0.15	0.17	0.42	0.000	0.320	0.22
	0.00	0.30	24.96	20.33	0.15	0.17	0.43	0.000	0.320	0.22
	0.00	0.30	25.20	20.30	0.15	0.16	0.43	0.000	0.330	0.22
Mean	0.00	0.33	25.04	20.32	0.15	0.17	0.42	0.000	0.320	0.22
C-03 D	1.87	0.98	13.50	64.98	0.15	1.90	1.63	0.760	0.050	3.56
	1.53	0.89	13.36	64.99	0.15	1.88	1.61	0.770	0.050	3.58
	1.57	0.82	13.32	64.71	0.15	1.89	1.61	0.760	0.050	3.55
Mean	1.66	0.89	13.39	64.89	0.15	1.89	1.61	0.760	0.050	3.56
C-01 C4	0.00	0.35	23.50	20.16	0.16	0.16	0.43	0.000	0.330	0.22
	0.00	0.33	23.55	20.15	0.15	0.16	0.43	0.000	0.320	0.22
	0.00	0.27	23.79	20.16	0.15	0.16	0.44	0.000	0.330	0.22
Mean	0.00	0.32	23.61	20.16	0.15	0.16	0.43	0.000	0.330	0.22
C-04 1	0.68	1.52	17.32	69.89	0.193	1.74	3.09	0.756	0.053	4.90
	0.28	1.49	17.49	70.01	0.178	1.76	3.05	0.749	0.060	5.05
	0.29	1.44	17.63	69.95	0.178	1.73	3.02	0.796	0.051	5.05
Mean	0.42	1.48	17.48	69.95	0.183	1.74	3.05	0.767	0.055	5.00
C-01 H/A	1.53	0.98	14.96	73.39	0.175	2.22	1.87	0.864	0.063	4.12
	1.63	0.99	14.82	73.43	0.175	2.20	1.86	0.876	0.063	4.13
	1.78	1.03	14.90	73.22	0.174	2.18	1.89	0.816	0.064	4.10
Mean	1.65	1.00	14.90	73.35	0.175	2.20	1.87	0.852	0.063	4.12
C-01 H/A	1.13	1.11	12.16	77.98	0.253	2.41	2.26	0.496	0.035	2.19
	1.27	1.18	12.11	77.83	0.264	2.37	2.27	0.506	0.036	2.20
	0.95	1.14	12.28	78.00	0.256	2.36	2.29	0.504	0.035	2.21
Mean	1.12	1.15	12.18	77.94	0.258	2.38	2.27	0.502	0.035	2.20
C-01 C3	1.52	1.18	11.83	77.68	0.236	2.27	2.53	0.542	0.040	2.23
	1.30	1.08	11.87	77.94	0.242	2.27	2.48	0.567	0.039	2.27
	1.47	1.19	11.90	77.61	0.234	2.26	2.48	0.542	0.043	2.33
Mean	1.43	1.15	11.87	77.74	0.237	2.27	2.50	0.551	0.041	2.27
C-01 C1/C2	1.60	0.98	16.06	72.33	0.168	2.05	1.52	0.834	0.058	4.57
	1.12	0.95	16.05	72.78	0.169	2.07	1.53	0.861	0.071	4.59
	1.20	0.99	16.05	72.68	0.169	2.05	1.53	0.869	0.059	4.58
Mean	1.31	0.98	16.05	72.60	0.169	2.06	1.53	0.855	0.063	4.58
C-01 A	1.61	1.27	16.80	71.05	0.172	1.98	1.84	0.801	0.057	4.57
	1.38	1.28	16.81	71.24	0.172	1.97	1.85	0.801	0.059	4.58
	1.28	1.15	16.82	71.43	0.173	1.97	1.83	0.804	0.054	4.60
Mean	1.42	1.23	16.81	71.24	0.172	1.97	1.84	0.802	0.057	4.58
C-01 D	1.25	1.03	12.67	76.88	0.203	2.31	2.46	0.507	0.039	2.68
	1.25	1.08	12.57	76.89	0.187	2.29	2.49	0.527	0.040	2.73
	1.49	1.08	12.71	76.62	0.219	2.35	2.38	0.491	0.037	2.66
Mean	1.33	1.06	12.65	76.80	0.203	2.31	2.44	0.508	0.039	2.69
C-01 G	1.53	1.10	16.42	71.76	0.167	1.99	1.27	0.916	0.069	4.97
	1.38	0.99	16.23	72.29	0.168	1.97	1.24	0.898	0.071	4.96
	1.63	1.19	16.28	71.74	0.167	2.01	1.26	0.924	0.062	4.93
Mean	1.51	1.09	16.31	71.93	0.167	1.99	1.26	0.913	0.067	4.96
C01 F	1.13	1.00	11.27	79.01	0.214	2.19	2.46	0.452	0.041	2.25
	1.19	0.98	11.15	79.10	0.216	2.20	2.44	0.447	0.044	2.25
	0.90	1.01	11.23	79.18	0.203	2.18	2.56	0.427	0.046	2.28
Mean	1.07	0.99	11.22	79.10	0.211	2.19	2.49	0.442	0.044	2.26
C-01 G	1.37	1.25	16.59	71.43	0.17	2.02	1.43	0.836	0.060	5.00
	1.45	1.08	16.51	71.58	0.17	1.99	1.43	0.844	0.060	5.04
	1.54	1.14	16.59	71.39	0.169	2.02	1.39	0.871	0.060	5.00
Mean	1.45	1.16	16.56	71.47	0.170	2.01	1.42	0.850	0.060	5.01
C-01 I	1.59	1.27	12.13	76.87	0.192	2.34	2.85	0.452	0.036	2.29
	1.26	1.23	11.97	77.35	0.192	2.37	2.86	0.479	0.032	2.29
	1.52	1.22	12.05	77.03	0.192	2.39	2.86	0.474	0.035	2.26
Mean	1.46	1.24	12.05	77.08	0.192	2.37	2.85	0.468	0.034	2.28
C-01 J	1.60	1.48	16.61	70.90	0.175	1.93	2.07	0.747	0.048	4.57
	1.21	1.36	16.74	71.27	0.176	1.91	2.07	0.747	0.053	4.60
	1.34	1.36	16.65	71.19	0.175	1.91	2.08	0.759	0.050	4.61
Mean	1.38	1.40	16.67	71.12	0.175	1.92	2.07	0.751	0.050	4.59

(continued on next page)

Table 2 (*continued*)

Sub-op unit[a]	Na_2O	MgO	Al_2O_3	SiO_2	P_2O_5	K_2O	CaO	Ti	MnO	Fe_2O_3
C-01 K	1.39	1.28	11.68	78.04	0.203	2.29	2.42	0.427	0.034	2.25
	1.48	1.17	11.56	78.14	0.189	2.29	2.42	0.476	0.033	2.27
	1.38	1.21	11.66	78.09	0.189	2.30	2.42	0.469	0.035	2.29
Mean	1.42	1.22	11.64	78.09	0.194	2.29	2.42	0.457	0.034	2.27
C-01 I	1.70	1.42	12.78	75.82	0.186	2.35	2.66	0.522	0.035	2.56
	1.46	1.39	12.82	76.10	0.187	2.34	2.60	0.531	0.040	2.59
	1.49	1.41	12.85	76.06	0.187	2.34	2.57	0.517	0.035	2.59
Mean	1.55	1.41	12.82	76.00	0.187	2.35	2.61	0.523	0.037	2.58
UR-01 1	0.90	1.43	16.58	71.09	0.174	2.13	2.82	0.799	0.060	4.16
	0.73	1.26	16.49	71.45	0.174	2.16	2.85	0.798	0.057	4.18
	0.74	1.29	16.50	71.41	0.179	2.14	2.85	0.814	0.055	4.18
Mean	0.79	1.33	16.52	71.31	0.176	2.15	2.84	0.804	0.057	4.17
C-02 1	1.28	1.30	14.75	73.28	0.228	2.74	2.54	0.739	0.054	3.21
	1.20	1.31	14.89	73.15	0.235	2.74	2.57	0.752	0.054	3.20
	1.33	1.35	14.99	72.93	0.241	2.75	2.52	0.751	0.053	3.19
Mean	1.27	1.32	14.87	73.12	0.235	2.74	2.54	0.747	0.054	3.20
C-02 2	1.35	1.63	15.83	70.31	0.248	2.38	4.11	0.634	0.042	3.57
	1.41	1.52	15.74	70.45	0.234	2.41	4.09	0.652	0.046	3.55
	1.14	1.38	15.60	70.94	0.205	2.44	4.13	0.671	0.049	3.57
Mean	1.30	1.51	15.72	70.57	0.229	2.41	4.11	0.652	0.046	3.56
C-02 3A	1.49	1.26	16.76	70.05	0.178	2.19	2.75	0.761	0.057	4.64
	1.75	1.43	16.93	69.52	0.176	2.16	2.74	0.727	0.058	4.63
	1.54	1.49	17.01	69.56	0.175	2.14	2.77	0.761	0.051	4.64
Mean	1.59	1.39	16.90	69.71	0.176	2.16	2.75	0.750	0.055	4.64
C-02 4	2.16	1.94	16.92	69.90	0.179	1.97	1.80	0.701	0.051	4.51
	1.85	1.74	16.73	70.66	0.180	1.99	1.76	0.691	0.050	4.48
	1.93	1.53	16.47	71.03	0.182	1.97	1.73	0.716	0.047	4.53
Mean	1.98	1.74	16.70	70.53	0.180	1.98	1.76	0.702	0.049	4.51
C-02 5	1.99	1.59	14.79	72.78	0.186	2.18	2.65	0.666	0.040	3.23
	1.68	1.50	14.54	73.36	0.187	2.19	2.66	0.677	0.044	3.24
	1.66	1.40	14.51	73.48	0.189	2.21	2.67	0.671	0.050	3.24
Mean	1.78	1.50	14.61	73.21	0.187	2.19	2.66	0.671	0.045	3.24
C-02 6	1.60	1.65	12.71	76.68	0.198	2.25	1.91	0.544	0.037	2.49
	1.44	1.49	12.49	77.18	0.197	2.27	1.90	0.524	0.035	2.53
	1.84	1.38	12.24	77.14	0.198	2.25	1.89	0.536	0.038	2.53
Mean	1.63	1.51	12.48	77.00	0.198	2.26	1.90	0.534	0.037	2.52
C-02 7A	1.81	2.03	16.42	70.40	0.178	2.20	2.09	0.756	0.058	4.18
	1.79	1.82	16.18	70.81	0.179	2.21	2.06	0.774	0.060	4.25
	1.85	1.85	16.03	70.84	0.180	2.24	2.07	0.769	0.060	4.24
Mean	1.81	1.90	16.21	70.68	0.179	2.22	2.08	0.766	0.059	4.22
C-02 7B	1.67	1.32	12.60	77.31	0.193	2.29	1.67	0.566	0.036	2.39
	1.65	1.37	12.71	77.20	0.191	2.27	1.65	0.577	0.033	2.39
	1.88	1.46	12.83	76.72	0.190	2.31	1.69	0.551	0.033	2.38
Mean	1.73	1.39	12.71	77.08	0.191	2.29	1.67	0.565	0.034	2.39
C-02 7 D	1.84	1.46	12.92	76.56	0.190	2.27	1.56	0.579	0.047	2.63
	1.70	1.46	13.04	76.59	0.189	2.27	1.57	0.556	0.046	2.62
	1.88	1.44	13.14	76.39	0.189	2.23	1.55	0.561	0.047	2.62
Mean	1.81	1.45	13.03	76.51	0.189	2.26	1.56	0.565	0.047	2.63
C-02 7E	1.75	1.81	15.09	72.82	0.184	2.20	2.09	0.704	0.048	3.42
	1.54	1.72	14.86	73.26	0.186	2.22	2.11	0.717	0.054	3.46
	1.65	1.62	14.79	73.29	0.187	2.21	2.12	0.712	0.048	3.49
Mean	1.65	1.72	14.91	73.12	0.186	2.21	2.11	0.711	0.050	3.45
A-09 1	0.79	1.34	17.27	69.95	0.183	2.36	2.80	0.781	0.057	4.62
	0.62	1.30	17.33	69.99	0.202	2.35	2.85	0.781	0.056	4.66
	0.53	1.20	17.45	70.00	0.197	2.35	2.87	0.798	0.056	4.69
Mean	0.65	1.28	17.35	69.98	0.194	2.35	2.84	0.786	0.056	4.66
A-09 2	0.84	1.02	14.21	75.39	0.190	2.26	2.54	0.529	0.038	3.05
	1.07	1.10	14.23	75.09	0.188	2.23	2.54	0.547	0.039	3.02
	0.89	1.08	14.50	74.96	0.188	2.24	2.59	0.524	0.038	3.04
Mean	0.93	1.07	14.31	75.15	0.189	2.24	2.56	0.533	0.038	3.04
A-09 3	1.08	1.21	14.06	75.41	0.205	2.14	2.39	0.532	0.041	2.99
	1.03	0.93	13.94	75.86	0.195	2.16	2.31	0.539	0.038	3.06
	1.05	0.93	13.88	75.82	0.195	2.17	2.35	0.537	0.041	3.08
Mean	1.05	1.02	13.96	75.70	0.198	2.16	2.35	0.536	0.040	3.04
A-09 4	1.21	0.99	14.87	74.54	0.183	2.32	2.15	0.597	0.042	3.16
	1.42	1.09	14.88	74.22	0.183	2.34	2.14	0.611	0.044	3.16
	1.31	1.12	14.91	74.26	0.200	2.34	2.11	0.614	0.041	3.16
Mean	1.32	1.07	14.89	74.34	0.189	2.33	2.13	0.607	0.042	3.16
A-09 5	1.00	1.05	15.76	72.23	0.176	2.24	2.86	0.769	0.060	3.98
	1.09	1.05	15.90	72.05	0.176	2.23	2.82	0.781	0.055	3.98
	1.03	1.15	16.02	71.86	0.204	2.25	2.84	0.791	0.060	3.94
Mean	1.04	1.08	15.89	72.04	0.185	2.24	2.84	0.780	0.058	3.97
A-09 6	0.91	1.15	15.73	73.55	0.205	2.17	2.35	0.596	0.048	3.38
	0.83	1.07	15.54	73.83	0.189	2.23	2.36	0.584	0.048	3.40
	0.74	1.06	15.44	74.05	0.189	2.25	2.33	0.606	0.052	3.38

(*continued on next page*)

Table 2 (*continued*)

Sub-op unit[a]	Na_2O	MgO	Al_2O_3	SiO_2	P_2O_5	K_2O	CaO	Ti	MnO	Fe_2O_3
Mean	0.82	1.09	15.57	73.81	0.194	2.21	2.35	0.595	0.049	3.39
A-09 7B	0.78	1.45	14.11	74.83	0.193	2.01	2.76	0.519	0.039	3.37
	0.90	1.21	13.70	75.40	0.196	2.03	2.71	0.537	0.043	3.35
	1.12	1.22	13.60	75.38	0.196	2.01	2.69	0.504	0.039	3.31
Mean	0.93	1.29	13.80	75.20	0.195	2.01	2.72	0.520	0.040	3.35
A-09 8	0.97	0.81	8.95	84.06	0.199	1.59	1.27	0.392	0.031	1.76
	0.86	0.75	8.99	84.20	0.201	1.66	1.18	0.370	0.026	1.78
	0.87	0.74	8.94	84.17	0.202	1.69	1.18	0.412	0.027	1.81
Mean	0.90	0.77	8.96	84.14	0.201	1.65	1.21	0.392	0.028	1.79
A-09 9	1.87	1.78	15.44	72.01	0.177	2.28	1.91	0.824	0.049	3.81
	2.07	1.87	15.48	71.73	0.174	2.29	1.89	0.783	0.043	3.80
	1.73	1.67	15.44	72.28	0.176	2.31	1.89	0.784	0.047	3.80
Mean	1.89	1.77	15.45	72.01	0.176	2.29	1.89	0.797	0.046	3.80
A-09 11	2.05	1.57	14.15	74.33	0.182	2.32	1.95	0.634	0.040	2.85
	1.76	1.49	14.12	74.73	0.183	2.36	1.91	0.634	0.038	2.84
	1.72	1.40	14.00	74.98	0.184	2.35	1.92	0.619	0.041	2.84
Mean	1.85	1.49	14.09	74.68	0.183	2.34	1.92	0.629	0.040	2.84
A-09 10	2.62	2.17	15.04	70.32	0.179	2.31	2.94	0.757	0.054	3.74
	2.54	2.03	14.90	70.54	0.180	2.32	3.01	0.778	0.055	3.78
	2.55	1.90	14.90	70.69	0.181	2.30	3.01	0.778	0.059	3.77
Mean	2.57	2.03	14.95	70.51	0.180	2.31	2.99	0.771	0.056	3.77
A-09 12	2.07	1.83	16.53	70.42	0.174	2.02	1.17	0.871	0.065	5.02
	1.90	1.85	16.53	70.56	0.174	2.05	1.18	0.873	0.063	5.00
	1.93	1.78	16.40	70.73	0.175	2.04	1.18	0.879	0.065	5.01
Mean	1.97	1.82	16.49	70.57	0.174	2.04	1.18	0.874	0.064	5.01
A-09 13	1.90	1.77	16.06	71.21	0.174	2.12	1.37	0.859	0.058	4.64
	2.01	1.64	15.97	71.31	0.174	2.12	1.38	0.888	0.059	4.61
	1.97	1.54	15.90	71.57	0.175	2.10	1.39	0.844	0.057	4.62
Mean	1.96	1.65	15.98	71.37	0.174	2.12	1.38	0.864	0.058	4.62
A-09 14	2.22	1.74	15.96	70.74	0.172	2.09	1.93	0.863	0.060	4.41
	1.92	1.54	15.96	71.17	0.173	2.12	1.94	0.846	0.057	4.44
	1.51	1.47	15.93	71.68	0.175	2.13	1.94	0.839	0.058	4.44
Mean	1.88	1.58	15.95	71.20	0.173	2.11	1.94	0.849	0.058	4.43
A-09 15	2.91	2.07	14.71	71.25	0.195	1.82	2.31	0.614	0.043	4.17
	2.94	1.90	14.63	71.36	0.197	1.79	2.42	0.579	0.048	4.21
	2.89	1.86	14.40	71.66	0.198	1.81	2.42	0.604	0.044	4.21
Mean	2.91	1.94	14.58	71.42	0.197	1.81	2.38	0.599	0.045	4.20

[a] The first designation refers to the sub-op and the second to the soil unit.

4.2. Age of the ash falls

If the anomalously high levels volcanogenic mineral phenocrysts were admixtures, which originated from multiple catastrophic volcanic events dating sometime between 0.639 ± 0.002 and 2.059 ± 0.004 Ma, then we should expect to find high levels of Ni, Cr, and Pt ubiquitously distributed stratigraphically in Chaco Canyon. However, their occurrence is not omnipresent, but concentrated in three contemporaneous, or near-contemporaneous, late Holocene strata.

In the Dune Dam area, anonymously high levels of Ni and Cr and volcanogenic mineral phenocrysts were identified in three-late Holocene strata (C-03 B, C-03 C2, and C-01 C4, Fig. 10) within an ancestral Puebloan canal identified by Vivian (1972). AMS radiocarbon and an OSL ages were obtained from stratum C4, a berm constructed during a modification of the canal. The age determinations were 985 ± 20 yr. B.P. (800–953 cal. yr. B.P., 997–1150 CE; Tankersley et al., 2017) and 978 ± 60 yr. B.P. (918–1038 yr. B.P., 976–1096 CE), respectively. These ages overlap with the proposed initial volcanic eruptions of Sunset Crater and the Pueblo II cultural period (Hanson et al., 2008a; Hanson et al., 2008b; Elson et al., 2011a; Elson et al., 2011b; Hanson, 2017).

4.3. Impact on Ancestral Puebloan culture

Initially, a volcanic ash fall could have been detrimental to Ancestral Puebloan hydraulic systems such as canals and reservoirs by potentially clogging and infilling them with an airborne sediment. Volcanic ash could have also been harmful to pollenating insects, fouled aquatic resources, and caused short-term damage to terrestrial plant and animal foods. Such negative consequences were likely ameliorated by distance, which would have diminished potential damaging impacts on vegetation (Martin et al., 2009; De Shutter et al., 2015).

Aside from the real and perceived dangers to Ancestral Puebloans from a late Holocene volcanic eruption and ash fall, there would have been significant benefits. For example, a late Holocene volcanic ash fall would have helped sustain soil fertility (e.g., Shoji et al., 1993; Shoji, 2006) and potentially fueled Ancestral Puebloan population growth and sustainability in Chaco Canyon (see Tankersley, 2017:381). Additionally, volcanic ash would have been highly valued as a raw material for tempering pottery (e.g., Tankersley et al., 2011, 2015, 2016b).

Although it has never been investigated, late Holocene volcanic ash was likely collected throughout Chaco Canyon and the greater San Juan Basin and stored following an eruption. The ash would have been very easy for Ancestral Puebloans to collect and stockpile in large quantities. While volcanogenic mineral temper has been well documented in

Table 3
Trace elements content (ppm) of sediment from the Chaco Wash, Escavada Wash, and Rincons.

Alluvium	As	Ba	Co	Cr	Cu	Nb	Ni	Pb	Rb	Sr	Th	U	V	Y	Zn	Zr
Rincon 1	9	719	15	43	47	29	34	23	98	235	13	20	127	23	70	233
	8	719	15	12	51	23	30	29	101	244	14	22	116	29	76	238
	9	714	15	24	54	26	36	22	96	247	11	13	108	32	72	244
Mean	9	717	15	26	51	26	33	25	98	242	13	18	117	28	73	238
Rincon 3	12	695	14	36	13	22	21	7	95	157	14	11	125	26	64	329
	8	679	14	59	15	25	25	21	104	158	14	24	123	22	67	340
	10	702	14	54	20	27	20	20	98	157	9	25	101	24	64	320
Mean	10	692	14	50	16	24	22	16	99	157	12	20	116	24	65	330
Rincon 4	9	1038	12	54	19	21	13	24	98	250	7	20	71	31	38	380
	10	1007	12	52	25	33	15	18	95	251	13	4	90	30	39	381
	10	1013	12	13	19	17	12	21	98	252	10	14	107	24	40	382
Mean	9	1019	12	40	21	24	13	21	97	251	10	13	89	29	39	381
Chaco F	8	968	12	67	22	22	17	24	96	250	14	23	88	31	43	351
	11	974	12	22	23	29	11	14	101	254	13	16	78	34	42	355
	8	980	12	28	25	19	14	26	100	245	11	18	94	29	43	347
Mean	9	974	12	39	23	24	14	21	99	249	13	19	87	31	43	351
Chaco G	8	797	17	67	43	26	10	21	84	204	13	12	171	22	71	263
	9	771	17	82	33	22	18	20	84	197	17	25	138	22	78	255
	7	817	17	101	36	23	30	26	80	195	14	21	119	23	75	252
Mean	8	795	17	83	37	24	19	22	83	199	15	19	142	22	75	257
Rincon 5	10	827	12	93	21	14	12	8	79	188	7	6	85	16	40	265
	11	831	12	78	18	18	12	12	91	192	15	20	102	17	45	275
	8	836	12	58	16	14	5	20	85	186	11	13	166	10	39	274
Mean	10	831	12	76	18	15	10	13	85	189	11	13	118	14	41	271
Escavada	9	816	12	75	19	20	5	16	82	188	12	19	75	22	45	306
3	9	821	12	50	20	14	17	14	81	187	11	14	88	17	42	310
	11	842	12	59	16	13	23	4	87	193	12	0	93	19	47	300
Mean	10	826	12	61	18	16	15	12	83	189	12	11	85	19	45	305
Chaco 1	9	689	16	32	52	29	24	20	95	223	16	12	155	29	81	204
	8	694	16	15	49	34	13	24	88	217	11	9	136	31	74	199
	10	677	16	33	52	38	17	21	97	221	12	18	85	33	72	208
Mean	9	687	16	27	51	34	18	21	93	220	13	13	126	31	75	204
Escavada	12	685	17	2	82	39	23	16	91	208	14	10	161	36	91	198
1	7	703	16	21	83	27	26	30	95	217	15	11	144	32	92	205
	8	671	16	44	76	38	23	26	99	221	15	14	118	34	89	202
Mean	9	686	16	22	80	35	24	24	95	215	15	12	141	34	90	202
Escavada	9	706	13	70	30	15	16	10	84	199	6	21	105	11	49	246
2	11	724	13	39	25	16	19	13	86	197	12	15	124	16	51	246
	11	701	13	84	21	22	23	14	88	207	7	15	110	18	46	249
Mean	10	710	13	64	25	18	19	12	86	201	8	17	113	15	49	247

ancient southwestern pottery (e.g., King, 2003), the frequency of late Holocene volcanic eruptions and the spatial and temporal pattern of associated ash temper use have not yet been examined and quantified.

5. Conclusions

Our investigations in Chaco Canyon, New Mexico provide the first evidence of volcanic ash fall in the four-corner region during the Pueblo II cultural period. Chaco Canyon provides an ideal location to examine the chronology and stratigraphy of volcanogenic mineral phenocrysts and their geochemistry. In addition to late Holocene alluvium, Chaco Canyon contains Ancestral Puebloan hydraulic features including a large suite of canals and reservoirs, which retain volcanogenic mineral phenocrysts from ash falls.

Scanning electron microscopy, energy-dispersive X-ray, energy dispersive X-ray fluorescence, inductively and coupled plasma spectrometry, and X-ray diffractometry demonstrate that the volcanic-derived minerals amphibole, apatite, biotite, clinopyroxene, epidote, ilmenite, olivine, smectite, and zircon are present in late Holocene sediments of the Dune Dam area of Chaco Canyon. AMS radiocarbon and OSL dating demonstrates that volcanogenic mineral phenocrysts were deposited sometime during the Pueblo II cultural period, ~1000–1100 CE. This age range overlaps with the proposed initial eruptions of Sunset Crater, Arizona. Volcanogenic mineral phenocrysts from this time period would be useful as a chronostratigraphic marker for other archaeological sites in the Southwest. At those sites where material for radiocarbon dating is rare or lacking, such volcanogenic markers, whether from Sunset Crater or from the Cascades, could be useful for first-order dating.

This natural occurrence of volcanogenic mineral phenocrysts has significant implications for understanding the Ancestral Puebloan exploitation of volcanic ash, landscape use, and sustainability. The

Table 4
Trace elements content (ppm) of sediments from the Dune Dam area.

Sub-op unit[a]	As	Ba	Co	Cr	Cu	Nb	Ni	Pb	Rb	Sr	Th	U	V	Y	Zn	Zr
C-03 L	6	697	10	42	20	22	26	17	74	173	11	4	98	16	40	464
	6	712	10	51	17	14	17	16	77	176	9	5	100	26	37	487
	6	700	10	43	15	15	7	14	77	183	9	5	72	20	38	488
Mean	6	703	10	45	17	17	17	16	76	177	10	4	90	21	39	480
C-03 B	5	0	18	1689	162	0	18698	7	0	1	7	9	155	0	145	31
	5	0	18	1662	142	6	18775	8	0	1	8	6	136	0	146	33
	5	0	18	1653	142	0	18677	4	0	1	5	2	123	0	142	30
Mean	5	0	18	1668	148	2	18717	6	0	1	7	6	138	0	144	31
C-03 C1	7	464	17	18	370	27	27	21	78	206	11	5	138	27	161	152
	7	481	17	63	379	20	16	24	74	209	5	0	131	26	158	157
	5	479	17	36	367	21	19	24	75	203	14	10	180	24	162	153
Mean	6	475	17	39	372	23	21	23	75	206	10	5	150	26	160	154
C-03 C2	7	0	20	1888	116	0	22040	2	0	2	5	2	146		144	33
	5	0	20	1905	108	0	22043	5	0	1	5	8	149		151	33
	5	0	20	1813	111	3	22004	7	0	1	6	13	142		137	31
Mean	6	0	20	1868	112	1	22029	5	0	1	5	7	146		144	32
C-03 D	5	648	13	14	30	30	19	26	83	213	12	0	126	27	62	243
	6	684	13	39	33	21	22	29	89	219	10	13	78	27	57	245
	5	671	13	60	34	29	13	31	91	219	12	7	84	25	64	248
Mean	5	668	13	37	32	27	18	29	88	217	11	7	96	26	61	245
C-01 C4	5	0	21	1887	84	1	23436	4	0	2	8	5	145		138	33
	5	0	21	1886	73	3	23458	9	0	2	8	7	131		138	33
	5	0	21	1851	80	2	23331	8	0	1	7	5	148		137	34
Mean	5	0	21	1875	79	2	23408	7	0	2	8	6	141		138	34
C-04 1	11	760	12	56	17	14	14	14	84	203	8	25	81	17	48	244
	9	786	12	67	13	15	21	18	87	207	7	10	79	13	43	235
	9	780	12	34	16	16	8	14	89	215	9	6	77	21	41	245
	10	775	12	52	16	15	14	15	86	208	8	13	79	17	44	241
C-01 H/	8	649	16	71	66	22	23	28	86	197	11	16	110	24	180	195
A	9	668	16	24	63	25	29	21	85	204	16	21	117	21	176	196
	9	688	16	23	62	22	21	20	89	204	15	18	174	27	179	203
Mean	8	668	16	39	63	23	24	23	86	202	14	18	134	24	178	198
C-01 H/	9	787	12	64	18	9	12	17	85	204	11	20	78	18	45	224
A	10	749	12	51	16	24	14	14	91	210	11	18	82	23	44	231
	9	763	12	21	16	17	21	21	81	198	15	0	114	11	41	220
Mean	9	767	12	45	17	17	16	17	86	204	12	13	91	18	43	225
C-01 C3	9	659	16	20	225	31	25	28	91	213	17	9	154	26	133	201
	7	650	17	19	224	24	29	27	95	214	16	11	151	34	125	202
	10	663	16	39	236	33	21	19	94	211	11	16	79	28	127	202
Mean	8	657	16	26	228	29	25	25	93	213	14	12	128	29	128	202
C-01 C1/	9	822	13	80	13	8	7	18	93	194	9	23	83	15	40	230
C2	13	815	13	61	23	14	11	6	95	197	12	19	133	13	37	234
	10	781	13	40	19	10	9	12	87	189	12	22	133	12	42	235
Mean	11	806	13	60	19	11	9	12	92	193	11	21	116	13	39	233
C-01 A	12	824	13	47	41	20	18	12	92	199	6	20	92	17	56	278
	10	776	13	60	49	11	17	16	90	203	8	10	98	16	57	281
	9	835	13	37	43	18	12	18	81	186	7	15	106	18	57	244
Mean	10	812	13	48	44	16	15	15	88	196	7	15	99	17	57	267
C-01 D	10	641	16	13	244	38	29	16	87	205	15	11	119	28	130	242
	8	674	16	18	243	25	24	26	94	214	16	19	163	30	124	250
	7	675	16	24	252	33	15	24	90	210	19	15	143	30	125	243
Mean	8	663	16	18	247	32	23	22	90	210	16	15	142	29	126	245
C-01 G	8	772	15	10	46	33	22	27	109	267	16	9	97	33	71	270
	9	784	15	38	40	28	21	24	100	251	11	5	97	30	79	255
	8	758	15	60	52	31	24	26	96	248	15	7	93	30	77	250
Mean	8	771	15	36	46	30	23	25	102	255	14	7	95	31	76	258
C-01 F	12	649	12	81	13	22	17	6	77	136	14	24	89	30	42	613
	9	656	12	81	8	23	25	14	78	135	11	14	86	24	40	630
	9	621	12	19	10	17	18	16	80	133	12	17	145	23	41	608
Mean	10	642	12	60	10	20	20	12	78	135	13	18	107	26	41	617
C-01 G	12	621	14	84	13	20	17	12	75	118	12	20	76	18	60	192
	10	640	13	31	16	20	17	17	76	116	17	19	132	19	60	193
	11	660	14	108	15	17	13	13	77	122	9	14	89	18	64	201
Mean	11	640	14	74	15	19	16	14	76	119	13	18	99	18	61	195
C-01 I	9	764	15	106	21	13	20	21	87	162	14	23	120	19	56	174
	11	748	15	112	14	18	20	12	82	156	15	16	76	18	52	168
	10	791	15	85	15	16	19	15	91	173	9	23	103	14	51	179
Mean	10	768	15	101	16	16	20	16	87	163	13	20	100	17	53	174
C-01 J	11	693	12	293	13	18	19	9	90	149	12	26	78	12	42	238
	9	718	12	247	12	18	15	11	88	154	16	13	79	16	44	245
	7	740	12	227	11	15	13	20	86	148	11	25	96	20	42	236
Mean	9	717	12	256	12	17	16	13	88	150	13	21	84	16	43	240

(*continued on next page*)

Table 4 (*continued*)

Sub-op unit[a]	As	Ba	Co	Cr	Cu	Nb	Ni	Pb	Rb	Sr	Th	U	V	Y	Zn	Zr
C-01 K	10	658	12	58	8	21	16	15	82	132	13	9	117	13	48	219
	9	620	12	61	13	11	17	10	81	135	8	15	76	16	54	221
	10	681	12	73	17	20	11	14	79	130	9	19	86	18	52	217
Mean	10	653	12	64	13	17	15	13	81	133	10	14	93	16	52	219
C-01 I	14	1012	13	56	23	34	18	7	100	259	7	11	72	33	44	368
	10	976	13	31	17	37	17	21	107	264	10	12	97	32	45	378
	11	1008	13	50	21	36	19	19	105	259	14	14	135	29	45	368
Mean	12	999	13	46	20	35	18	16	104	261	10	12	101	31	45	371
UR-1 1	9	799	13	59	15	24	10	21	93	206	15	32	89	27	58	315
	8	791	13	93	18	22	23	21	90	209	10	23	80	27	58	311
	8	798	13	85	19	27	13	22	82	191	11	14	112	28	56	286
Mean	8	796	13	79	18	24	15	22	88	202	12	23	93	27	57	304
C-02 1	8	843	13	42	37	24	22	27	98	210	16	16	74	26	69	376
	8	866	13	19	33	32	18	25	110	226	12	32	117	23	68	410
	7	852	13	59	35	23	18	27	102	220	13	11	133	28	66	396
Mean	8	854	13	40	35	26	19	26	103	219	14	20	108	26	68	394
C-02 2	8	622	15	56	29	19	18	24	84	180	18	7	85	20	65	279
	8	652	14	76	20	20	19	19	95	185	10	26	129	24	68	302
	8	632	14	58	25	27	26	24	87	176	10	25	104	24	66	274
Mean	8	636	14	63	25	22	21	22	88	180	13	19	106	23	66	285
C-02 3A	6	754	16	22	42	28	16	24	90	208	14	8	126	28	80	205
	10	798	16	41	41	23	18	20	92	203	13	11	153	26	81	199
	6	755	16	75	36	25	28	30	91	202	16	11	99	22	86	206
Mean	7	769	16	46	40	25	20	25	91	204	14	10	126	25	83	203
C-02 4	10	634	16	44	27	25	21	16	79	187	15	24	103	26	71	221
	10	603	16	65	35	18	26	17	92	189	11	32	116	22	76	242
	9	631	16	18	27	25	21	18	95	198	16	23	146	23	79	246
Mean	10	623	16	42	30	23	23	17	89	191	14	26	122	24	75	236
C-02 5	8	728	14	37	51	28	9	21	88	263	14	6	98	25	71	320
	7	731	14	36	48	17	20	26	100	281	16	22	114	21	71	334
	7	716	14	41	49	23	21	27	96	272	17	20	91	24	67	324
Mean	7	725	14	38	49	22	16	25	94	272	16	16	101	23	70	326
C-02 6	12	704	13	22	23	10	15	12	91	195	11	5	131	19	56	247
	9	739	13	43	15	18	21	16	87	184	12	25	81	19	47	248
	10	772	13	18	22	17	13	17	89	184	16	35	92	18	44	248
Mean	10	738	13	28	20	15	16	15	89	188	13	22	101	18	49	248
C-02 7A	7	787	15	2	67	17	24	25	95	218	11	19	140	26	81	239
	7	769	15	30	64	31	9	24	98	227	15	6	80	26	82	243
	12	778	15	3	62	34	27	19	106	233	13	18	96	37	87	252
Mean	9	778	15	12	64	28	20	23	100	226	13	14	105	30	83	244
C-02 7B	10	819	12	67	26	17	20	19	95	224	14	28	79	29	47	305
	11	823	12	20	22	22	10	16	91	228	8	17	101	16	48	311
	10	797	12	20	20	18	21	11	95	219	8	26	102	22	50	306
Mean	10	813	12	35	23	19	17	16	94	224	10	24	94	23	48	307
C-02 7D	7	832	13	47	26	18	24	26	88	229	17	17	78	23	52	197
	7	844	13	37	25	18	17	20	90	236	14	14	119	18	48	204
	8	846	13	36	23	17	17	21	87	230	13	15	77	21	54	205
Mean	7	841	13	40	25	18	19	22	88	231	15	15	91	21	52	202
C-02 7E	9	741	14	41	53	26	14	21	89	193	10	23	95	24	70	242
	8	749	14	19	54	26	16	20	91	197	15	29	79	27	73	247
	10	753	14	51	48	26	22	15	94	203	9	22	101	25	71	258
Mean	9	748	14	37	52	26	17	19	91	198	11	25	92	25	71	249
A-09 1	8	674	16	2	39	25	21	23	97	202	17	27	159	26	84	289
	9	670	16	39	40	23	20	21	100	206	15	15	147	25	79	287
	7	693	16	84	43	21	17	26	98	212	16	6	114	28	83	288
Mean	8	679	16	42	41	23	19	24	98	207	16	16	140	26	82	288
A-09 2	10	731	13	40	40	14	14	16	91	186	13	29	77	20	68	176
	11	715	13	45	39	30	22	5	89	189	14	17	102	20	62	177
	9	720	13	30	41	10	17	12	98	190	9	32	155	9	67	181
Mean	10	722	13	38	40	18	18	11	93	188	12	26	111	17	66	178
A-09 3	7	712	14	16	42	17	13	18	88	183	12	17	140	15	68	208
	7	749	14	59	49	21	19	27	94	195	13	32	83	18	66	215
	10	733	14	58	41	16	9	15	86	189	18	3	103	13	65	206
Mean	8	731	14	44	44	18	14	20	89	189	14	17	108	15	66	210
A-09 4	10	745	13	54	59	27	23	19	92	200	12	14	95	22	80	247
	9	748	13	40	70	26	16	22	90	197	16	10	106	25	76	238
	10	736	13	36	60	29	21	12	93	197	11	18	96	21	75	237
Mean	10	743	13	43	63	27	20	18	92	198	13	14	99	23	77	241
A-09 5	9	692	15	53	48	25	17	17	96	221	15	28	108	30	78	383
	6	676	15	34	41	23	31	31	98	223	16	13	129	24	82	389
	9	733	15	2	50	31	21	20	94	226	16	17	109	31	84	380
Mean	8	700	15	29	46	26	23	23	96	223	16	19	116	28	81	384

(*continued on next page*)

Table 4 (*continued*)

Sub-op unit[a]	As	Ba	Co	Cr	Cu	Nb	Ni	Pb	Rb	Sr	Th	U	V	Y	Zn	Zr
A-09 6	11	675	14	65	39	14	25	11	83	157	15	31	76	19	71	226
	7	702	14	69	38	22	18	21	83	156	16	27	117	19	66	223
	10	694	14	67	46	17	11	15	82	153	9	33	77	19	72	220
Mean	10	690	14	67	41	18	18	16	82	155	13	30	90	19	70	223
A-09 7B	9	617	15	35	33	17	8	16	79	153	13	17	108	16	62	196
	9	630	14	71	26	15	18	16	75	143	15	29	119	22	67	190
	8	599	14	52	27	11	10	25	78	151	9	26	98	15	64	200
Mean	9	615	14	52	29	14	12	19	77	149	12	24	108	18	64	195
A-09 8	8	596	11	63	21	14	8	14	61	110	14	20	114	8	31	171
	7	582	11	79	23	21	0	17	61	121	15	15	94	10	39	182
	9	559	12	60	21	4	14	14	66	116	13	24	114	10	38	189
Mean	8	579	12	67	22	13	7	15	63	115	14	20	107	9	36	181
A-09 9	8	803	15	43	43	29	17	22	92	231	13	12	101	30	80	314
	9	772	14	59	49	30	23	23	91	228	19	19	99	33	80	315
	8	780	14	50	52	36	10	24	96	231	13	31	138	30	79	309
Mean	9	785	14	51	48	32	17	23	93	230	15	21	113	31	80	313
A-09 11	7	813	13	100	30	27	18	26	96	243	17	27	92	27	71	263
	11	809	13	105	33	14	20	16	98	240	14	35	123	21	75	257
	6	815	13	96	40	15	18	24	103	261	15	26	115	23	77	282
Mean	8	813	13	100	34	19	19	22	99	248	16	30	110	24	74	267
A-09 10	9	772	15	62	55	23	13	19	91	294	10	0	101	31	70	293
	11	777	14	4	51	34	28	17	94	287	11	22	132	31	70	296
	9	773	14	22	50	25	19	23	99	315	14	16	74	28	78	315
Mean	10	774	14	29	52	27	20	20	95	299	12	13	102	30	73	301
A-09 12	11	640	17	24	60	26	17	21	101	228	17	20	136	27	101	212
	9	659	17	40	58	35	17	21	97	226	18	23	180	26	106	213
	11	659	16	47	58	28	14	16	104	230	13	33	132	30	89	216
Mean	10	653	17	37	59	30	16	19	101	228	16	26	149	28	98	214
A-09 13	9	728	16	38	51	29	21	23	100	248	13	18	148	33	88	225
	8	717	16	31	46	37	22	24	101	251	16	19	165	35	82	224
	9	694	16	35	43	25	29	25	96	245	11	27	136	33	84	224
Mean	9	713	16	35	47	30	24	24	99	248	14	22	150	33	84	224
A-09 14	9	667	15	45	52	33	20	22	101	299	22	29	101	32	91	219
	8	642	15	47	51	31	17	25	100	304	18	30	131	32	93	226
	11	675	15	2	55	38	17	16	97	304	15	21	132	28	92	220
Mean	9	662	15	31	53	34	18	21	99	302	18	27	122	31	92	222
A-09 15	12	666	16	50	48	24	20	17	78	174	10	15	95	25	76	163
	9	661	16	17	43	17	31	20	78	186	13	16	137	18	78	173
	7	678	16	39	46	16	18	32	86	192	17	21	129	25	71	175
Mean	10	668	16	35	45	19	23	23	81	184	13	17	120	23	75	170

[a] The first designation refers to the sub-op and the second to the soil unit.

presence and mineralogical composition of airborne volcanic minerals supports the position that Ancestral Puebloans living in Chaco Canyon had a local source of volcanic ash that was well suited for temper in the production of pottery. Ancestral Puebloans living in Chaco Canyon and the greater San Juan basin would have found it very easy to collect volcanic ash. Volcanic-derived mineral temper has been well documented in ceramics at Chaco Canyon and the San Juan Basin.

Although it is beyond the scope of this paper, the mineralogical and geochemical data presented in this paper might be used to help determine the geographic extent and chronology of late Holocene ash fall in the greater San Juan basin, which could be compared to chronological patterns in ceramic tempering. In addition to providing important raw materials needed in the production of pottery, volcanic ash would have also enhanced the fertility of agricultural soils in Chaco Canyon.

Volcanic eruptions and associated earthquakes during the Pueblo II period likely had religious implications and possibly resulting in traditional oral histories. The main-shock earthquake associated with a late Holocene volcanic eruption may have dislodged boulders and smaller rocks from the canyon walls thus threatening human life, residences, kivas, and material culture. In Hopi emergence stories, earthquakes are associated with incessant fighting, decadence, and a threat that the earth would swallow those who did not flee. Hopi oral histories tell of cataclysmic earthquakes destroying an entire Pueblo for misbehaving during a ceremony, improperly performing a ceremony, or abandoning sacred rituals (Wallis, 1936). Earthquakes are also thought to occur if the *Bálölöokong* (water serpents), which live in springs and provide water are not properly honored (Voth, 1905).

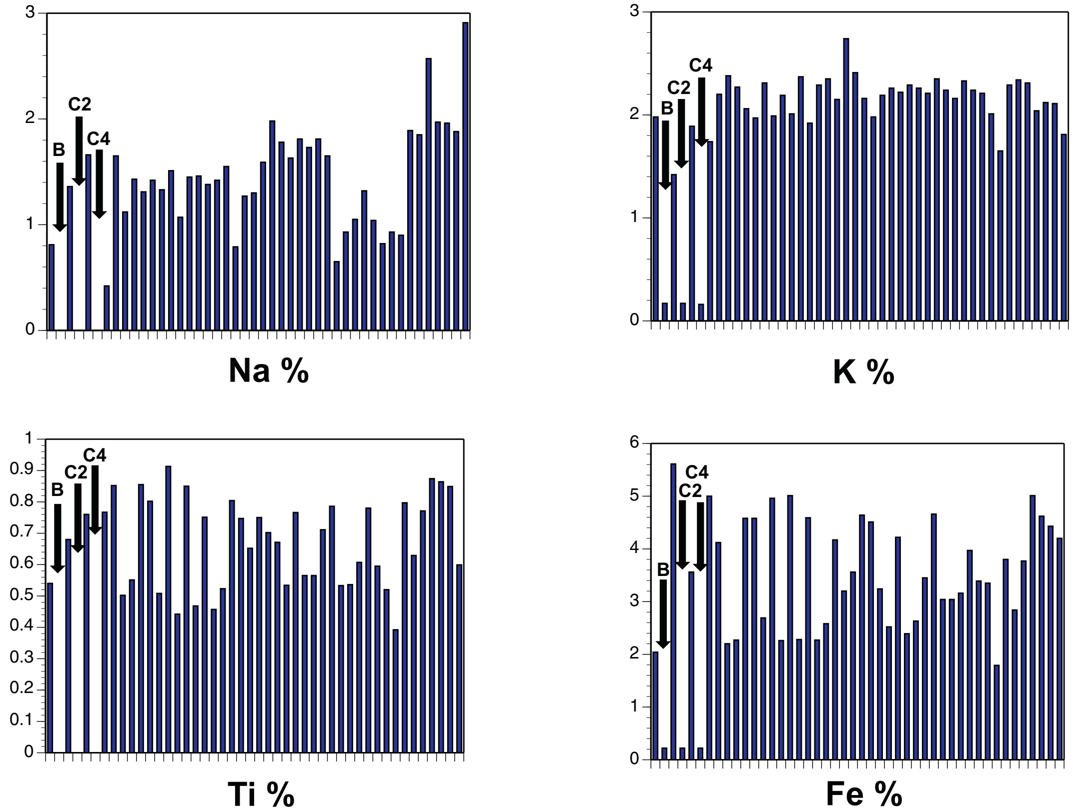

Fig. 7. Minor element percent composition of sediments from the Dune Dam area illustrating the paucity of Na, K, Ti, and Fe in strata B, C2, and C4.

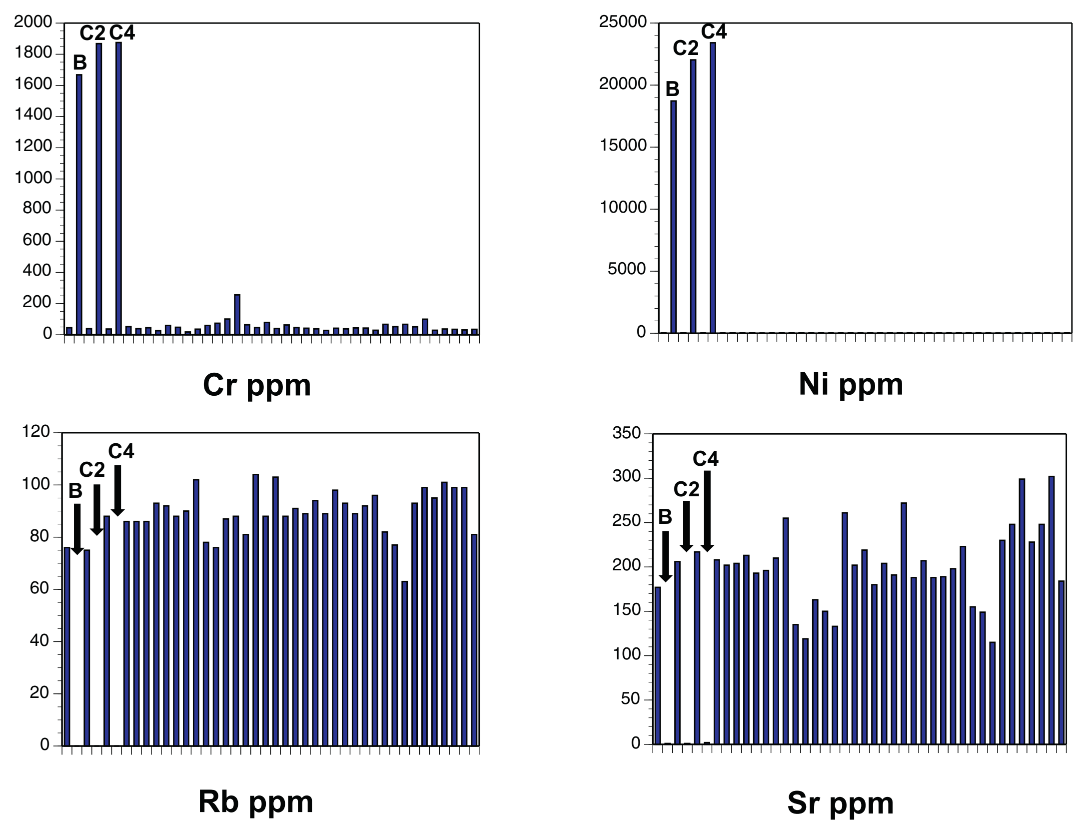

Fig. 8. Trace element percent composition of sediments from the Dune Dam area illustrating the robust quantity of Cr and Ni and the paucity of Rb and Sr in strata B, C2, and C4.

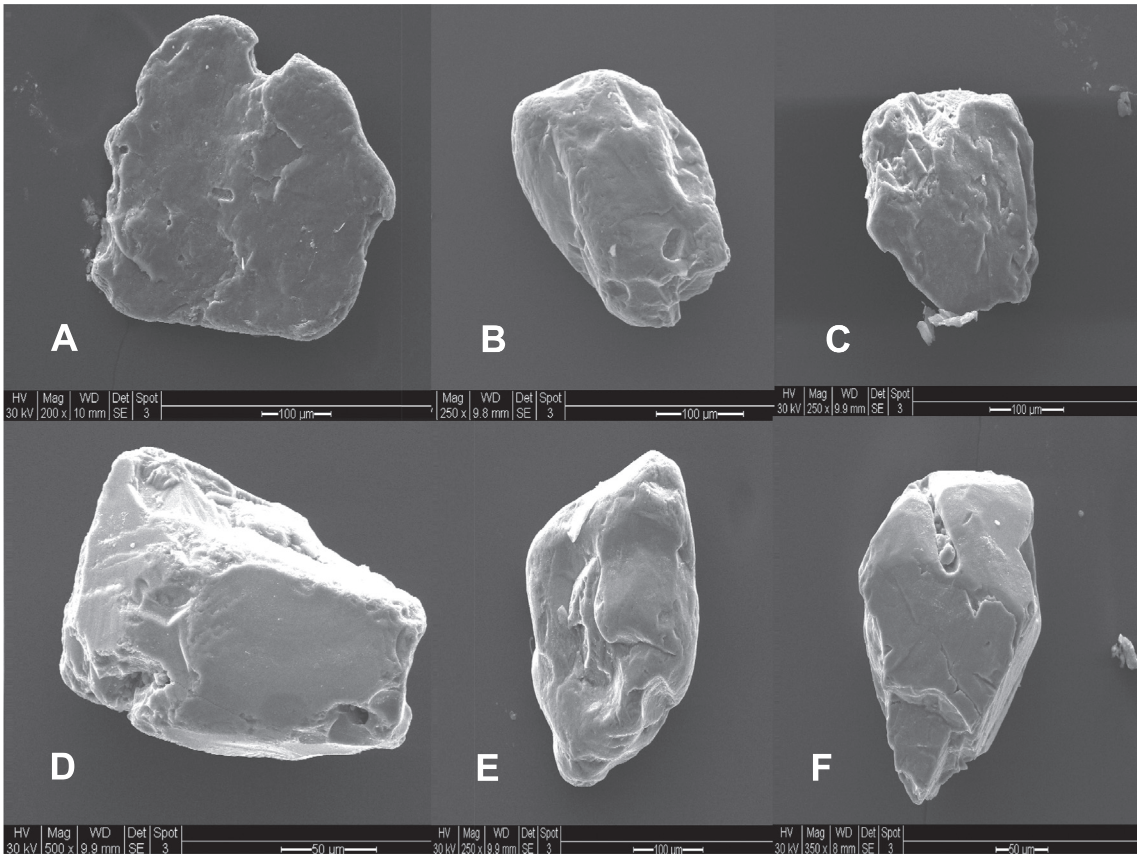

Fig. 9. Environmental scanning electron micrographs of volcanogenic minerals from sediments in the Dune Dam area: A. amphibole, B. biotite, C. Epidote, D. Ilmenite, E. Olivine, F. Zircon.

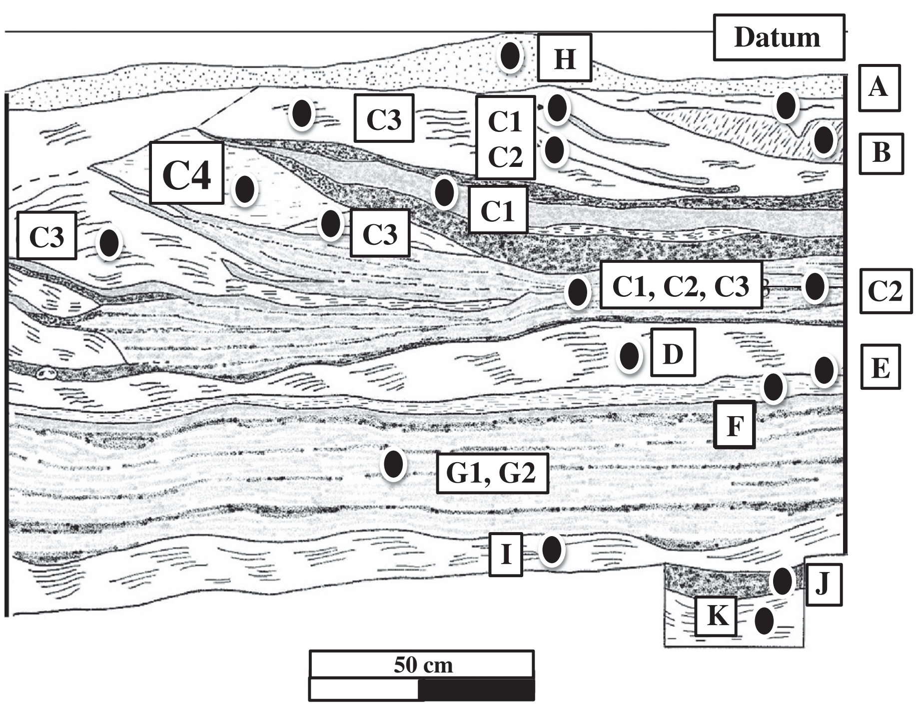

Fig. 10. Excavation profile of Op. C-01. Unit C4 is a constructed berm. Units B, C1, C2, C3, D, F, G1, G2, J, and L are fluvial sediments or soil derived from fluvial sediment. Units E, H, and L are aeolian sediments or soil derived from those sediments. Unit A is a combination of fluvial and Aeolian sediment and a soil derived from those sediments.

Table 5
Identification and composition of volcanogenic minerals in sediments from Op C-01 C4.

Sample	Elemental composition[a]	Mineral
1	Fe, Ti, O	Ilmenite
2	Zr, Al, Si, O	Zircon
3	Ca, Fe, Al, Si, O	Epidote
4	Ti, Fe, Mn, O	Ilmenite
5	K, Mg, Fe, Al, Si, O	Biotite
6	K, Fe, Mn, Al, Co, Si	Amphibole
7	K, Mg, Fe, Al, Si, O	Biotite
8	Fe, Mn, Ti, Si, O	Olivine
9	Fe, Mn, Ti, Si, O	Olivine
10	Fe, Ti, O	Ilmenite
11	K, Mg, Fe, Al, Si, O	Biotite

[a] Identified by energy dispersive analysis of X-rays (EDAX).

Acknowledgments

This paper greatly benefitted from the contributions of our interdisciplinary Quaternary research team including Christopher Carr, Stephen Plog, Adam S. Watson, and graduate students Samantha G. Fladd, Katelyn J. Bishop, Jon Paul McCool, Jessica Thress, and Elizabeth Haussner. Funding from the University of Cincinnati Research Council, the Charles Phelps Taft Foundation, and the Court Family Foundation supported this study as well as the Dean of the College and Graduate School of Arts and Sciences of the University of Virginia. We are especially grateful to the National Park Service, Chaco Canyon National Historic Park, the New Mexico Office of Archaeological Studies, the Navajo Nation, members of the American Indian Advisory Council to the National Park Service, and Chaco Canyon National Historic Park. This work was accomplished under permit 15-CHCU-01. A key collaborative source for the success of this project has been Gwinn Vivian, and we wish to acknowledge his openness and generosity of mind and spirit. We wish to extend a special thanks to Paul Potter for his keen insights on the geologic contexts of minor and trace elements. The comments and suggestions of the reviewers and editors were helpful and much appreciated.

References

Bailey, R.A., Smith, R.L., Ross, C.S., 1969. Stratigraphic nomenclature of volcanic rocks in the Jemez Mountains, New Mexico. Geol. Den. Surv. Bull. 1274-P (23 p.).
Brindley, G.W., Brown, G. (Eds.), 1980. Crystal Structures of Clay Minerals and Their X-ray Identification. Mineralogical Society 41 Queen's Gate, London.
Christiansen, R.L., Blank Jr., H.R., 1972. Volcanic stratigraphy of the Quaternary rhyolite plateau in Yellowstone National Park. Geol. Surv. Prof. Pap. 279-B (28 p.).
Cully, A., Toll, M., 2015. Evaluation of agricultural potential on four additions to Chaco Culture National Historical Park. In: Powers, R.P., Van Dyke, R.M. (Eds.), The Chaco Additions Survey: An Archaeological Survey of the Additions to Chaco Culture National Historical Park, Reports of the Chaco Center, National Park Service, Chaco Research Archive. University of Virginia, Charlottesville.
De Shutter, A., Kervyn, M., Canters, F., Bosshard-Stadlin, S.A., Songo, M.A.M., Mattsson, H.B., 2015. Ash fall impact on vegetation: a remote sensing approach of the Oldoinyo Lengai 2007–2008 eruption. J. Appl. Volcanol. 4, 15.
Dean, J.S., Funkhouser, G., 2002. Appendix A: dendroclimatology and fluvial chronology in Chaco Canyon. In: Force, E.R., Vivian, R.G., Windes, T.C., Dean, J.S. (Eds.), Relations of "Bonito" Paleo-channels and Base-level Variations to Anasazi Occupation, Chaco Canyon, New Mexico. Arizona State Museum Archaeological Series 194 (Tucson).
Elson, M.D., Ort, M.H., Anderson, K.C., Heidke, J.M., Sheppard, P.R., Samples, T.L., 2011a. In: the shadow of the volcano: prehistoric settlement in the U.S. 89 Project Area. In: Elson, M.D. (Ed.), Sunset Crater Archaeology: The History of a Volcanic Landscape. Prehistoric Settlement in the Shadow of the Volcano. Anthropological Papers No. 37 Center for Desert Archaeology, Tucson, pp. 187–211.
Elson, M.D., Ort, M.H., Sheppard, P.R., Samples, T.L., Anderson, K.C., May, E.M., Street, D.J., 2011b. Sunset crater volcano. In: Elson, M.D. (Ed.), Sunset Crater Archaeology: The History of a Volcanic Landscape. Prehistoric Settlement in the Shadow of the Volcano. Anthropological Papers No. 37 Center for Desert Archaeology, Tucson, pp. 103–129.
Eveleth, R.W., Lueth, V.W., 2010. Gemstone deposits of the Four Corners region, USA. In: Fassett, J.E., Zeigler, K.E., Lueth, V.W. (Eds.), Geology of the Four Corners Country, New Mexico. Geological Society 61st Annual Fall Field Conference Guidebook.
Hanson, S.L., 2017. Sunset crater volcano: a cinder cone eruption that impacted the Ancestral Puebloan Indians. Ariz. Geol. April 9, 2–3.
Hanson, S.L., Duffield, W., Plescia, J., 2008a. Quaternary volcanism in the San Francisco volcanic field: recent basaltic eruptions that profoundly impacted the Northern Arizona landscape and disrupted the lives of nearby residents. In: Duebendorfer, E.M., Smith, E.I. (Eds.), Field Guide To Plutons, Volcanoes, Faults, Reefs, Dinosaurs, and Possible Glaciation, Selected Areas Of Arizona, California, and Nevada. Geological Society of America Field Guide 11. pp. 173–186.
Hanson, S.L., Falster, A.U., Simmons, W.B., 2008b. Mineralogy of fumarole deposits at Sunset Crater Volcano National Monument, Northern Arizona. Rocks Miner. 83 (6), 534–544.
Haussner, E.A., 2016. A Revised Middle to Late Holocene Alluvial Chronology of Chaco Canyon, New Mexico (Unpublished M.S. Thesis). Department of Geology, University of Cincinnati.
Haussner, E., Huff, W., Tankersley, K., 2015. Weathered Quaternary Tephras at Chaco Canyon National Historic Park, New Mexico. In: Poster Paper Presented at the Annual Meeting of the Geological Society of America, Baltimore, Maryland.
Hunt, A.M., Dvoracek, D.K., Glascock, M.D., Speakman, R.J., 2014. Major, minor, and trace element mass fractions determined using ED-XRF, WE-XRF, and INAA for five certified clay reference materials: NCS DC 60102-60105; NCS DC 61101 (GBW 03101A, 03102A, 03103, and 03115). J. Radiat. Chem. http://dx.doi.org/10.1007/s10967-01403266-z.
Ingham, M.N., Starbuck, P.H., 1995. Investigation of the suitability of Elvacite, used as a liquid binder, for the analysis of pressed powder samples by X-ray flouresence spectrometry. In: British Geological Survey. Analytical Geochemistry Series (Technical Report WI/94/5).
Izett, G.A., Wilcox, R.E., Powers, H.A., Desborough, G.A., 1970. The Bishop Ash Bed, a Pleistocene marker bed in the western United States. Quat. Res. 1, 121–132.
Judd, N.M., 1954. The Material Culture of Pueblo Bonito. Smithsonian Institution, Publication 4172, Washington, D.C.
Kelley, D.H., Milone, E.F., 2004. Exploring Ancient Skies: An Encyclopedic Survey of Archaeoastronomy. Springer.
King, V.C., 2003. The Organization of Production of Chuska Gray Ware Ceramics for Distribution and Consumption in Chaco Canyon, New Mexico (Ph.D. dissertation). Department of Anthropology, University of New Mexico, Albuquerque.
Lekson, S.H., 2005. The Archaeology of Chaco Canyon: An Eleventh-Century Pueblo. Regional Center. School of Advanced Research Press, Santa Fe, New Mexico.
Marshall, M.P., Stein, J.R., Loose, R.W., Novotny, J.E., 1979. Anasazi Communities of the San Juan Basin. Public Service Company of New Mexico, Albuquerque, and the New Mexico Historic Preservation Bureau, Santa Fe.
Martin, R.S., Watt, S.F.L., Pyle, D.M., Mather, T.A., Matthews, N.E., Georg, R.B., Day, J.A., Fairhead, T., Witt, M.L.I., Quayle, B.M., 2009. Environmental effects of Ashfall in Argentina from the 2008 Chaitén volcanic eruption. J. Volcanol. Geotherm. Res. 188, 462–472.
Moore, C.R., West, A., LeCompte, M.A., Brooks, M.J., Daniel Jr., I.R., Goodyear, A.C., Ferguson, T.A., Ivester, A.H., Feathers, J.K., Kennett, J.P., Tankersley, K.B., Victor Adedeji, A., Bunch, T.E., 2017. Widespread platinum anomaly documented at the Younger Dryas onset in North American sedimentary sequences. Nat.: Sci. Rep. 7, 44031. http://dx.doi.org/10.1038/srep44031. www.nature.com/scientificreports.
Plog, S., 2012. Ritual and cosmology in the Chaco Era. In: Glowacki, D.M., Van Keuren, S. (Eds.), Religious Transformations in the Late Pre-Hispanic Pueblo World. University of Arizona Press, Tucson, pp. 50–65.
Schreiber, H.D., 1979. Experimental studies of nickel and chromium partitioning into olivine from synthetic basaltic melts. In: Lunar and Planetary Science Conference, 10th, Houston, Tex., March 19–23, 1979, Proceedings. vol. 1. Pergamon Press, Inc., New York, pp. 509–516.
Scott, G.R., O'Sullivan, R.B., Weide, D.L., 1984. Geological Map of the Chaco Culture National Historic Park, Northwestern New Mexico. United States Geological Survey, Reston, Virginia.
Shackley, M.S., 2011. X-ray Fluoresence Spectrometry (XRF) in Geoarchaeology. Springer Press, New York.
Shoji, S., 2006. Factors of soil formation: Climate, as exemplified by volcanic ash soils. In: Certini, G., Scalenge, R. (Eds.), Soils: Basic Concepts and Future Challenges. Cambridge University Press, Cambridge, pp. 131–149.
Shoji, S., Nanzyo, M., Dahlgren, R.A., 1993. Volcanic Ash Soils: Genesis, Properties, and Utilization. Elsevier, Amsterdam.
Strutin, M., 1994. Chaco: A Cultural Legacy, Southwest Parks and Monuments Association. Southwest Parks & Monuments Association, Tucson.
Tankersley, K.B., 2017. Geochemical, economic and ethnographic approaches to the evaluation of soil, salinity, and water management in Chaco Canyon, New Mexico. J. Archaeol. Sci. Rep. 12, 378–383.
Tankersley, K.B., Scarborough, V.L., Dunning, N., Huff, W., Maynard, B., Gerke, T.L., 2011. Evidence for volcanic ash fall in the Maya Lowlands from a Reservoir at Tikal, Guatemala. Journal of Archaeol. Sci. 38, 2925–2938.
Tankersley, K.B., Dunning, N., Scarborough, V.L., Carr, C., Jones, J., Lentz, D., 2015. Fire and water: the archaeological significance of Tikal's Quaternary sediments. In: Lentz, David (Ed.), The Archaeology of Tikal. Cambridge University Press, pp. 186–211.
Tankersley, K.B., Dunning, N.P., Thress, J., Owen, L.A., Huff, W.D., Fladd, S.G., Bishop, K.J., Plog, Watson, A.S., Carr, C., Scarborough, V.L., 2016a. Evaluating soil salinity and water management in Chaco Canyon, New Mexico. J. Archaeol. Sci. Rep. 9, 94–104.
Tankersley, K.B., Dunning, N.P., Scarborough, V.L., Huff, W.D., Lentz, D., Carr, C., 2016b. Catastrophic volcanism and its implication for agriculture in the Maya Lowlands. J. Archaeol. Sci. Rep. 5, 465–470.
Tankersley, K.B., Owen, L.A., Dunning, N.P., Fladd, S.G., Bishop, K.J., Lentz, D.L., Slotten, V., 2017. Micro-flotation removal of coal contaminants from archaeological radiocarbon samples from Chaco Canyon, New Mexico, USA. J. Archaeol. Sci. Rep. 12,

66–73.
Vivian, R.G., 1972. Prehistoric water conservation in Chaco Canyon. In: Final Technical Report to the National Science Foundation, Grant No. GS-3100, Washington, D.C.
Vivian, R.G., 1990. The Chacoan Prehistory of the San Juan Basin. Academic Press, New York.
Vivian, R.G., Hilpert, B.E., 2012. The Chaco Handbook. University of Utah Press, Salt Lake City.
Vivian, R.G., Watson, A.S., 2015. Reevaluating and modeling agricultural potential in the Chaco Core. In: Heitman, C.C., Plog, S. (Eds.), Chaco Revisited: New Research on the Prehistory of Chaco Canyon, New Mexico. University of Arizona Press, Tucson, pp. 30–65.
Vivian, R.G., Van West, C.R., Dean, J.S., Akins, N., Toll, M., Windes, T., 2006. Appendix B: Chacoan ecology and economy. In: Lekson, S.H. (Ed.), The Archaeology of Chaco Canyon: An Eleventh-Century Pueblo Regional Center. School of American Research Press, Santa Fe, pp. 429–457.
Voth, H.R., 1905. The Traditions of the Hopi. Publications of Field Columbian Museum, Chicago.
Wallis, W.D., 1936. Folk tales from Shumopovi, Second Mesa. J. Am. Folk. 49 (191–92), 17–18.
Wilcox, R.E., Naeser, C.W., 1992. The Pearlette Family ash beds in the Great Plains: finding their identities and their roots in the Yellowstone Country. Quat. Int. 13/14, 9–13.
Wills, W.H., Dorshow, W.B., 2012. Agriculture and community in Chaco Canyon: revisiting Pueblo Alto. J. Anthropol. Archaeol. 31 (2), 138–155.